NASA TECHNICAL MEMORANDUM

NASA TM X-3240

NASA TM X-3240

DESCRIPTION AND INITIAL OPERATING PERFORMANCE OF THE LANGLEY 6-INCH EXPANSION TUBE USING HEATED HELIUM DRIVER GAS

John A. Moore

Langley Research Center
Hampton, Va. 23665

NATIONAL AERONAUTICS AND SPACE ADMINISTRATION • WASHINGTON, D. C. • SEPTEMBER 1975

1. Report No.	2. Government Accession No.	3. Recipient's Catalog No.
NASA TM X-3240		

4. Title and Subtitle	5. Report Date
DESCRIPTION AND INITIAL OPERATING PERFORMANCE OF THE LANGLEY 6-INCH EXPANSION TUBE USING HEATED HELIUM DRIVER GAS	September 1975
	6. Performing Organization Code
7. Author(s)	8. Performing Organization Report No.
John A. Moore	L-9900
	10. Work Unit No.
9. Performing Organization Name and Address	502-27-01-02
NASA Langley Research Center Hampton, Va. 23665	11. Contract or Grant No.
	13. Type of Report and Period Covered
12. Sponsoring Agency Name and Address	Technical Memorandum
National Aeronautics and Space Administration Washington, D.C. 20546	14. Sponsoring Agency Code

15. Supplementary Notes

16. Abstract

A general description of the Langley 6-inch expansion tube is presented along with discussion of the basic components, internal resistance heater, arc-discharge assemblies, instrumentation, and operating procedure. Preliminary results using unheated and resistance-heated helium as the driver gas are presented. Driver-gas pressure ranged from approximately 17 to 59 MPa and temperature ranged from 300 to 510 K. Test-gas–acceleration-gas interface velocities of approximately 3.8 to 6.7 km/sec were generated using air as the test gas and helium as the acceleration gas. Test flow quality and comparison of measured and predicted expansion-tube flow quantities are discussed.

17. Key Words (Suggested by Author(s))	18. Distribution Statement
Impulse facility Hypervelocity Expansion tube Shock wave	Unclassified – Unlimited Subject Category 09

19. Security Classif. (of this report)	20. Security Classif. (of this page)	21. No. of Pages	22. Price*
Unclassified	Unclassified	40	$3.75

*For sale by the National Technical Information Service, Springfield, Virginia 22161

DESCRIPTION AND INITIAL OPERATING PERFORMANCE OF THE LANGLEY 6-INCH EXPANSION TUBE USING HEATED HELIUM DRIVER GAS

John A. Moore
Langley Research Center

SUMMARY

A general description of the Langley 6-inch expansion tube is presented along with discussion of the basic components, internal resistance heater, arc-discharge assemblies, instrumentation, and operating procedure. Preliminary results using unheated and resistance-heated helium as the driver gas are presented. Driver-gas pressure ranged from approximately 17 to 59 MPa and temperature ranged from 300 to 510 K. Air was employed as the test gas and helium, as the acceleration gas.

The incident shock velocity in the driven section was observed to exceed prediction from simple, real-air shock-tube theory for the present range of pressure ratio across the primary diaphragm and driver-gas temperature. Measured differences between shock velocities resulting from an unheated helium driver gas and velocities with a resistance-heated driver gas were significantly less than prediction. The test-gas–acceleration-gas interface was observed to initially accelerate, then attenuate, in traversing the acceleration section. Pitot-pressure surveys indicated a test core diameter of approximately one-half the tube diameter at the higher interface velocities. Test times were in good agreement with prediction, except at the lower interface velocities of this study. Measured wall static pressures generally agreed with predicted values based on a thermochemical equilibrium expansion of the air test gas. However, measured pitot pressures generally fell between predictions for an equilibrium expansion and for a frozen expansion.

INTRODUCTION

The feasibility of the expansion tube as a facility suitable for high-velocity flow research was demonstrated by tests performed in the Langley pilot model expansion tube and reported in reference 1. While these tests confirmed that measured flow velocity, thermodynamic properties, and test-flow duration were of the order predicted by simple theory (ref. 2), a number of undesirable features surfaced. For example, measured velocity profiles at the test section (ref. 3) indicated the flow core diameter was approximately 50 percent of the tube diameter (9.5 cm). Hence, extremely small models would be

required for testing. Also, as noted in reference 4, the unmachined, extruded tube walls of the pilot model probably affected the location of boundary-layer transition, which in turn may have a detrimental effect on test-section flow quality. The poor repeatability of test conditions observed in reference 1 can be attributed, in part, to (1) a vacuum system plagued by leaks and (2) the randomness of the pressure ratio across the single primary diaphragm at rupture. However, the advantages from these pilot-model tests were judged to outweigh the disadvantages (ref. 1), thereby leading to the construction of a larger, more refined expansion tube.

The Langley 6-inch expansion tube offers a number of advantages over the pilot model, such as (1) smooth (machined) tube walls, (2) all stainless-steel construction, (3) larger tube diameter, (4) double primary diaphragm mode of operation, (5) increased pressure range for driver section, (6) improved vacuum system and greater pumping capability, and (7) much larger quantity of stored electrical energy for arc discharge. Design and construction were oriented to make this facility capable of producing the high velocities required for real-gas studies related to planetary entries with reasonable run frequency.

The primary purpose of this report is twofold. First, to present a general description of the Langley 6-inch expansion tube, along with discussion of the basic components, internal resistance heater, arc-discharge assemblies, instrumentation, and operating procedure. Second, to present preliminary results using unheated and resistance-heated helium as the driver gas. Test-flow quality and comparison of measured and predicted expansion-tube flow quantities are also discussed.

SYMBOLS

The International System of Units (SI) (ref. 5) are used for all physical quantities.

a	speed of sound, m/sec
M_s	incident-shock Mach number, U_s/a
p	static pressure, Pa
p_t	pitot pressure, Pa
T	temperature, K
U	velocity, m/sec

U_s incident-shock velocity, m/sec

x distance along tube, measured downstream from the primary diaphragm, m

Subscripts:

1 initial state in intermediate or driven section

4 initial state in driver section

5 state of test gas flow

10 initial state in acceleration section

DESCRIPTION AND OPERATION

Before discussing the basic components and operating procedure of the Langley 6-inch expansion tube, a brief introduction to the facility will be presented. This facility is basically a cylindrical tube divided into three sections by a primary diaphragm and a secondary diaphragm. As shown in figure 1, the primary diaphragm separates the driver or high-pressure section from the driven or intermediate section; the secondary diaphragm separates the driven section from the acceleration section. This acceleration section exits inside a large dump tank, and test models are positioned at the exit.

Prior to a run, the three sections and dump tank are evacuated. A gas having a high speed of sound, such as helium, is introduced into the driver section. The speed of sound may be increased by heating the driver gas with a 3-MW resistance heater or an electric-arc heater having either a coaxial or parallel-rail arrangement. The test gas, which is arbitrary, is introduced into the driven section; and the acceleration gas, generally helium, is introduced into the acceleration section and dump tank. A detailed discussion of the theoretical expansion-tube flow sequence is presented in reference 2.

Description of Basic Components

The Langley 6-inch expansion tube shares the Langley hot gas radiation research facility with the Langley 6-inch shock tube (ref. 6). This enables much of the supporting mechanical and electrical equipment to be shared by both tubes.

A sketch of the Langley 6-inch expansion tube is given in figure 2. The basic components of this facility are (1) the high-pressure driver section, (2) the intermediate or driven section, (3) the acceleration or expansion section, and (4) the dump tank.

Photographs of these components are shown in figure 3. Auxiliary equipment required for operation of the facility consists of (1) storage bottles for high-pressure driver gases, (2) high-pressure pump, (3) mechanical and diffusion pumps for evacuation of the various sections, (4) a resistance heater with power supply to heat the driver gas, and (5) capacitor banks and charging unit. These banks store electrical energy for the coaxial and parallel-rail electric-arc discharge units which are used to heat the driver gas to temperatures in excess of those possible with the resistance heater. Each of the basic components and the auxiliary equipment will now be described in more detail.

Driver section.- The driver section was designed as a pressure vessel capable of withstanding a maximum pressure of 138 MPa. A great deal of attention was given to the sealing of this section due to the difficulty of containing high-pressure helium and hydrogen driver gases. (The proposed use of hydrogen as a driver gas ushered in stringent safety requirements which were applied to all phases of design and construction.) This vessel was fabricated from ASTM A336 Type F8-304 stainless steel. The internal diameter is 35.6 cm and the section is 2.44 m long. This diameter will accommodate a resistance heater, the coaxial electric-arc assembly, or the parallel-rail electric-arc assembly. To reduce the quantity of driver gas required for unheated or resistance-heated mode of operation, a liner may be installed having a diameter of 16.5 cm. A breech plug with interrupted threads accepts the heaters and the electric-arc assemblies and seals the upstream end of the vessel.

Double-diaphragm section.- The transition between the driver section and driven section is achieved with the double-diaphragm section illustrated in figure 4. This section can accept either a single diaphragm, or two diaphragms spaced 15.24 cm apart. The entrance piece, square piece, and square-to-circular transition piece (fig. 4) are fabricated of 17-4 PH (condition H-1150) stainless steel.

An experimental study of the opening process of large steel diaphragms (ref. 7) showed that a ring flange was required to prevent the diaphragm from pulling in from the clamped edges. The diaphragms used in the present tests are sketched in figure 5. These diaphragms were machined from 304 stainless steel with a retaining ring flange integral with the diaphragm. Two diagonal grooves were machined in the face of each diaphragm 90° to each other at a depth required for a particular burst pressure.

The impact of the four diaphragm petals on the walls of the double-diaphragm section resulted in deformation of the walls, as well as occasional loss of the tips of the petals. These problems were alleviated by installing brass damper pads just downstream of the diaphragms to absorb the impact of the petals. This pad is four sided and has a thickness of 3.18 mm. Pad life is approximately 8 to 10 runs.

Driven section.- The most upstream section of the driven tube is fabricated from 17-4 PH (condition H-1150) stainless steel and designed for a maximum pressure of 69 MPa.

This section, which may be removed laterally to provide easy access to the double-diaphragm section, is 2.44 m long and has an internal diameter of 15.24 cm. As indicated in figure 2, the driven section length can be extended by adding additional sections, thereby requiring relocation of the secondary diaphragm. The test gas is introduced into this section prior to the run. The interior wall surface of all driven and acceleration (discussed subsequently) sections was machined to a 32-microinch finish.

Acceleration section.- The acceleration tube is made up of several sections of tubing that are 15.24 cm in internal diameter and of lengths 0.49, 2.14, or 4.57 m. These sections were fabricated from ASTM A314 Type 304 stainless steel and designed for a maximum pressure of 34.5 MPa. The total length of the acceleration section may be varied, with the maximum length used to date being 19.2 m. This ability to vary acceleration section length, resulting in a corresponding variation in driven section length (for this study, these two sections have a fixed, total length of 21.6 m), is a result of the run-time optimization study of reference 2.

A thin (generally mylar) diaphragm separates the driven and acceleration sections. The acceleration gas, which was helium in the present study, is introduced into the acceleration section prior to the run.

Dump tank.- The dump tank is a vessel 10.7 m long with an internal diameter of 1.22 m and a volume of approximately 12.8 m^3. This vessel is fabricated from 304 stainless steel and designed for a maximum pressure of 1.02 MPa and a minimum pressure of 0.0013 Pa. The expansion tube enters the upstream end of the dump tank through a slip joint and ends approximately 0.6 m into the tank. Model testing is performed at the exit of the expansion tube; hence, models are tested in an open jet. Schlieren quality windows of 45.7-cm diameter are located on opposite sides of the dump tank for viewing the flow about test configurations. Plates on the top and bottom of the dump tank provide bases for model support systems and header boxes, which serve as a means of exit for instrumentation leads from the test section.

Vacuum pumping system.- A rotary Roots blower type vacuum pump is used for initially evacuating the dump tank and acceleration section and driven section. A bypass line around the diaphragm separating the driven tube and acceleration tube helps to equalize the pressure in these two sections during pump down, thereby preventing rupture of the thin diaphragm. Two 50.8-cm diffusion pumps are used to obtain a minimum pressure of less than 0.01 Pa. This level of vacuum is necessary to minimize contaminants which will mix with the acceleration gas after it is entered into the acceleration section. Small mechanical pumps evacuate the driver section and driven section to approximately 7 Pa and 1 Pa, respectively. At the completion of each run, gases within the facility are dumped into a previously evacuated sphere having a diameter of 5.5 m. A two-stage steam ejector pump

is used to exhaust any potentially hazardous gases (such as hydrogen) remaining within the facility. This ejector pump is also used for sphere evacuation.

High-pressure system.- The high-pressure driver gases are stored in a bottle field consisting of 10 bottles with a total volume of 0.77 m^3. These bottles, which are external to the building and encircled by a wall of earth, are designed to withstand a pressure of 83 MPa. A diaphragm type pump, designed for 138 MPa, is used to transfer the gas from lower pressure bottles or a trailer to the storage field.

Resistance heater.- As discussed in reference 8, several studies have concluded that operational characteristics of resistance heating have significant advantages over other methods. Hence, this mode of heating the driver gas was incorporated into the design of the Langley 6-inch expansion tube. Three different size internal resistance heater elements were fabricated (ref. 8). Figure 6 illustrates the unit used for the present study, in which the driver-section diameter was 16.5 cm. The heating element (fig. 6) is constructed of two parallel modified Y-shaped stainless-steel (type 321) extrusions. These are connected at the upstream end to the 3-MW power supply by water-cooled beryllium-copper rods (alloy 10), which also mechanically restrain the element, and at the downstream end by two stainless-steel crossover plates. The two members of the element are separated from each other by H-shaped aluminum-oxide insulators and insulated from the driver wall by aluminum-oxide cylinders. A more detailed description of the heater, power supply, and performance of this heating unit is given in reference 8.

Electric-arc heating.- Two assemblies for heating the driver gas with an electric-arc discharge were designed and fabricated. One is a coaxial design (fig. 7(a)) and the other is a parallel-rail system (fig. 7(b)). The coaxial arrangement offers the advantage of fewer problems in the electrical and mechanical design. However, this arrangement results in longitudinal temperature gradients within the driver section since the electrodes are positioned at the upstream end of the section. A more uniform temperature distribution is expected from the parallel-rail design.

The energy to drive either of these systems is stored in a 10-MJ energy storage system consisting of four banks of capacitors and a charging unit. Each bank consists of 800 capacitors; each capacitor is rated at 12 000 V and 43 μF of capacitance. Groups of 10 capacitors are connected through a coaxial cable which leads to a coaxial collector (fig. 2). One collector serves each bank of 800 capacitors. This permits the bank to be used separately or in parallel with the other banks.

Operating Procedure

The theory of operation is given in reference 2 and the sequence of events is, briefly (see fig. 1):

(1) The driver section is pressurized to the desired level and the steel diaphragms separating the driver and driven sections are ruptured.

(2) The resulting incident shock wave travels into the quiescent test gas in the driven section and impacts and ruptures the thin diaphragm separating the driven and acceleration sections.

(3) A second incident shock travels through the quiescent acceleration gas.

(4) The test gas is accelerated through an unsteady expansion fan at the entrance of the acceleration section to the test velocity, pressure, and temperature at the test section (tube exit).

There are three procedures available for raising the driver pressure and rupturing the steel diaphragms separating the driver and driven sections. The first procedure uses an electric-arc discharge with a single steel diaphragm separating the two sections. The driver supply gas is introduced into the driver section until the desired pressure is obtained. Energy transferred to this gas by the electric-arc discharge raises the temperature and pressure high enough to insure rupture of the diaphragm.

The second procedure is generally used for unheated driver-gas operation with two steel diaphragms installed in the double-diaphragm section between the driver and driven sections. As the high-pressure supply gas is introduced into the driver section, it is also introduced into the volume between the two steel diaphragms. This double-diaphragm section is pressurized to approximately one-half the final driver pressure. To initiate diaphragm rupture, the gas between the two steel diaphragms is vented to atmosphere, thereby increasing the pressure difference across the upstream diaphragm. This overpressure ruptures the upstream diaphragm and allows the full pressure of the driver to rupture the second diaphragm. Such a method permits control of the ratio of driver-gas pressure to driven-gas pressure for a given run. The volume between the two diaphragms is small, being less than 7 percent of the total volume of the driver, and does not appreciably affect the final pressure ratio. A single diaphragm may also be used with this unheated driver-gas mode of operation.

The third procedure uses the resistance heater to raise the temperature of the driver gas, and is essentially the same procedure as used for the unheated driver-gas mode of operation; that is, when the desired pressure and temperature in the driver gas are obtained with the heater, the diaphragm rupture is initiated by venting the double-diaphragm section.

The driver, driven, and acceleration sections are evacuated prior to filling with the appropriate gases. Any gas or mixture of gases desired as a test medium may be introduced into the driven tube. The quiescent test-gas pressure is generally 0.3 to 17 kPa, although several tests have been performed for higher values of p_1. The acceleration gas provides a means of controlling the velocity and pressure (routinely measured quantities) of the test gas as it moves through the acceleration section. As noted in reference 2, a gas with low

molecular weight such as helium permits the use of higher initial acceleration-section pressure p_{10}. The same value of test-gas velocity and pressure obtained with the light acceleration gas may also be obtained with heavier acceleration gases, provided the quiescent densities of the two gases are equal (ref. 9). In the present study, helium was used as the acceleration gas and p_{10} was varied from roughly 3 to 930 Pa. To assure purity of the acceleration gas, it was stored in a pressure vessel mounted on the dump tank and introduced into the dump-tank acceleration section just prior to pressurization of the driver section and subsequent diaphragm rupture.

INSTRUMENTATION

Pressure

The expansion tube is characterized by extremely short test times. In general, the test time is less than 400 μsec, and thus the pressure instrumentation must have very fast response to pressure change and a minimum of orifice-cavity volume to reduce pressure-lag effects. Presently, stagnation pressure behind a normal shock (pitot pressure), model surface pressure, and expansion-tube wall pressure are measured with miniature piezoelectric (quartz) transducers having rise times of approximately 1 to 3 μsec and a pressure range of approximately 700 Pa to 20 MPa. The pressure transducers are used in conjunction with a charge amplifier, and the output signal is filtered and recorded from an oscilloscope with the aid of a camera. Representative oscilloscope films of pitot-pressure and wall-static-pressure traces are shown in figure 8. The maximum uncertainties in pressure measurements are believed to be less than ±20 percent for tube wall pressure and for pitot pressure (ref. 9).

Since piezoelectric transducers exhibit a zero shift when subjected to a positive temperature pulse, a coating of Pliobond or silicone RTV rubber was applied to the sensing surface of all transducers for thermal protection. Pressure transducers facing into the flow, such as used in the pitot-pressure survey-rake probes shown in figure 9, must be protected from steel slivers from the rupture line of the primary diaphragms and mylar fragments from the secondary diaphragm, carried in the posttest flow. The procedure used to protect these transducers was to employ an overlapping baffle arrangement just ahead of the transducer sensing surface (fig. 9). This arrangement did not introduce significant lag, as observed from the pitot-pressure response of figure 8, and successfully protected all pitot-probe transducers used in the present study.

Velocity

One method used to infer the incident shock velocity in the driven section and test-gas–acceleration-gas interface velocity in the acceleration section was the microwave technique (ref. 10). This microwave interferometer system is designed to introduce microwave energy

into the expansion tube, excite a standing wave in the tube due to reflection from the primary diaphragm, and then detect the movement of this standing wave due to the movement of the incident shock wave generated upon diaphragm rupture. The varying periodic signal is recorded on a high-speed (60 rps) drum-camera-oscilloscope combination and a representative microwave film for air test gas is shown in figure 8.

The antenna for this system consisted of an uninsulated tin-copper wire having a diameter of 0.61 mm. This wire was stretched vertically across the tube diameter and positioned approximately 5 cm downstream of the tube exit (fig. 3(d)). The signal generator was adjusted to put out a 1.33-GHz signal. This frequency results in the distance between successive minimums or successive maximums of the microwave trace (fig. 8) corresponding to a movement of 22.71 cm. Since 5.08 cm of film length corresponds to 1 msec, the time, hence corresponding velocity, between successive minimums or maximums is readily obtained.

If the electron density of the shock front or interface is not sufficient to provide reflection of the microwave signal, other techniques must be employed. A second, and somewhat more conventional means used to determine incident shock velocity was to position high response instrumentation along the length of the tube at known intervals. This procedure allows a position-time history to be generated; hence, the average velocity is determined between successive instrumented stations. The time interval for incident shock arrival between stations was determined from the response of piezoelectric pressure transducers, thin-film resistance heat-transfer gages, and photomultipliers mounted along the tube and flush with the tube wall. These three types of instrumentation produced sharp jumps in signal output upon shock arrival. Outputs from these types of instrumentation were recorded from an oscilloscope with the aid of a camera, and representative oscilloscope traces for pressure transducer, heat-transfer gage, and photomultiplier are presented in figure 8. Times for the shock to travel between stations were obtained by manually reading the oscilloscope film. Each type of instrumentation yields information about the flow behind the shock wave. With the exception of the pressure instrumentation, their present use was confined to determining time of arrival of the shock wave or the test-gas–acceleration-gas interface. For this study, the uncertainties in incident shock velocity in the driven section and interface velocity in the acceleration section are believed to be less than ±5 percent.

The locations of instrumentation stations along the tube used in this study are given in table 1. Since the facility was modified immediately after the present shakedown tests, the more recent locations of instrumentation are also tabulated in table 1 for future reference.

Schlieren System

The schlieren system used for this facility is a single pass, Z-shaped system using 40.65-cm-diameter f/6 parabolic mirrors, and 40.65-cm-diameter schlieren quality windows. Two recording systems may be used simultaneously. The first system uses a xenon arc lamp, with a pulse-forming network, as a source and an ultrahigh-speed framing camera to record the images. The duration of the light source can be selected as 60 μsec, 250 μsec, or 1000 μsec. With the range of framing rates of the high-speed camera, exposure times from 1 to 15 μsec can be obtained. This system is described in detail in reference 11. The second system uses a 200-nsec duration spark source. A still camera having a film size of 10.2 cm X 12.7 cm is used for recording. An electromagnetically collapsed aluminum-foil shutter, with an open-to-shut time of roughly 50 μsec, is used to prevent unwanted exposure from light produced in the posttest flow.

The single-exposure spark source system was alined on-axis to obtain the accuracy needed for shock-shape studies. The other system was alined slightly off-axis, and small, flat, front-surface mirrors were used to prevent interference of the two systems. A representative schlieren photograph taken with the single-exposure spark source system is shown in figure 10. This photograph illustrates the shock detachment distance for a flat-faced cylinder model in Mach 7.7 airflow at a normal shock density ratio of approximately 11.

Triggering System

Reliable triggering of facility instrumentation for an expansion tube is of primary concern. In the course of this shakedown, it was found that a reliable triggering signal for the oscilloscopes was produced by an accelerometer mounted to the outside surface of the double-diaphragm section. This accelerometer detected an acceleration in the axial direction of the tube resulting from the diaphragm rupturing process. For the present study, the signal from this accelerometer triggered oscilloscopes used to monitor the microwave signal and the output of pressure, heat transfer, and photomultiplier gages. Time delays to oscilloscopes monitoring instrumentation further downstream of the primary diaphragm were supplied by a digital time delay generator and are known to within a microsecond. This triggering method is not subject to spurious signals, nor does it require gain adjustments for varying instrumentation outputs.

When the resistance heater was used to heat the driver gas, chromel-alumel thermocouples were installed on the heater element and in the region of the driver between the downstream end of the heater and the diaphragm. This latter thermocouple was used to determine the driver-gas temperature T_4 just prior to rupture of the primary diaphragm.

TEST CONDITIONS

Test results reported herein were obtained during the shakedown on the expansion tube and thus are preliminary. The driver gas was helium at either ambient temperature (300 K) or heated by the resistance heater to a temperature of 450 to 510 K. Air was used as the test gas and helium, as the acceleration gas. The driven-section and acceleration-section lengths were 2.44 m and 19.2 m, respectively.

Test conditions for the present study, where T_1 is equal to 300 K, are given in table 2.

RESULTS AND DISCUSSION

Since the incident shock velocity in the driven section $U_{s,1}$ is a basic input to the computer program of reference 9, this quantity is measured routinely. A comparison of measured incident shock Mach number $M_{s,1}$ (equal to $U_{s,1}/a_1$) immediately upstream of the secondary diaphragm to prediction is shown in figure 11. Measured values of $U_{s,1}$ in the air test gas were determined from time-of-arrival gages. Due to the dependency of the microwave system on electron density (ref. 10), microwave traces were not always obtained, particularly at the lower velocities. When obtained, velocities inferred from the microwave traces were observed to be in good agreement with velocities inferred from time-of-arrival gages. Predicted values were obtained from the simple, real-air theory (that is, one-dimensional inviscid flow and a driven-to-driver cross-sectional area ratio of unity are assumed) of reference 9 for an imperfect helium driver gas over a range of driver-gas temperatures T_4. Experimental results for both unheated helium and resistance-heated helium driver gas are denoted in figure 11. The shaded symbols denote a test with a single diaphragm and open symbols denote double-diaphragm tests. For a given pressure ratio p_4/p_1, measured values of $M_{s,1}$ exceed predicted values for both unheated and heated driver gases. This discrepancy is attributed, in part, to the finite opening time of the heavy steel diaphragms (refs. 12 and 13). Although shock velocities for heated helium driver exceed velocities for unheated helium driver, the difference is significantly less than predicted; that is, for a given pressure ratio p_4/p_1, a 40- to 80-percent increase in helium-driver-gas temperature does not yield the expected (based on prediction) increase in performance. The results of figure 11 may imply an effect of the diaphragm mode of operation (single or double) for unheated helium driver gas and p_4/p_1 equal to 10 000· however, the few runs at this condition preclude a conclusion that higher shock velocities are generated with the double diaphragm.

The movement of the incident shock in the driven section and the test-air–helium-acceleration-gas interface velocity in the acceleration section, as inferred from microwave measurements, are illustrated in figure 12 for resistance-heated driver gas. It is interesting

to note that the shock velocity in the 2.44-m-long driven section is still accelerating upon arrival at the secondary diaphragm station. This trend of the incident shock initially accelerating is well established (refs. 12 and 14). According to predictions of reference 15, the helium acceleration gas behaves ideally (is not ionized) at the present flow conditions. Therefore, the helium acceleration gas should be transparent to the microwave signal, which thus tracks the interface. The interface is observed (fig. 12) to initially accelerate to a maximum velocity at about 20 tube diameters downstream of the secondary diaphragm, then attenuate with increasing distance from the secondary diaphragm. This attenuation between the station corresponding to the maximum velocity and the tube exit (approximately 14 m) is about 0.15 km/sec, which is of the same order as the attenuation reported for the pilot-model expansion tube over an 8-m length (ref. 1). The trend of attenuation in interface velocity was observed for all test conditions.

The incident shock velocity in the helium acceleration gas was determined from time-of-arrival gages. Attenuation of this shock is greater than the interface attenuation, starting out at a velocity about 10 percent higher than the interface velocity and ending at the test section at about the same velocity as the interface. This phenomenon is expected (ref. 16) and is due to viscous (tube-wall boundary-layer) effects.

Wall static pressure upstream of the tube exit (station 13, table 1) and pitot pressure at the test section are compared with theory in figure 13. Values of measured pitot pressure presented in figure 13 are the average of the pitot pressure measured with the two inner probes on either side of the centerline (see fig. 9). The computer program of reference 9 was used to determine theoretical values of the wall static and pitot pressures for a range of interface velocities. Measured shock velocity $U_{s,1}$ at the secondary diaphragm was used as input to determine the real-air thermochemical equilibrium conditions behind this shock (region ② of fig. 1), and an unsteady expansion was performed to a number of interface velocities in order to generate the curves of figure 13. The four different flow models (ref. 9) used in this comparison were designated "ISEE," "ISFE," "SSEE," and "SSFE," the notation being as follows:

(1) The incident shock in the test air does not reflect from the secondary diaphragm. This model is indicated by the notation IS, for incident shock.

(2) The incident shock reflects from the secondary diaphragm resulting in a standing normal shock immediately upstream of the diaphragm station. This model is indicated by the notation SS, for standing shock.

(3) The test air is assumed to be in thermodynamic equilibrium as it undergoes an unsteady expansion caused by the rupture of the secondary diaphragm. This state is designated by the notation EE.

(4) The vibrational energy and the chemistry of the test air remain unchanged (frozen) as the test air undergoes the unsteady expansion. This state is indicated by the notation FE.

Along with these four theoretical flow models plotted in figure 13 is a fifth model which assumes no shock reflection at the secondary diaphragm, assumes an equilibrium expansion, and includes the effect of attenuation of the test air velocity by ΔU_5 = -150 m/sec. The procedure for accounting for the effect of attenuation in the interface velocity is discussed in detail in reference 1. It should be noted that the region above the curve designated ISEE with ΔU_5 = -150 m/sec represents the predicted existence of thermochemical equilibrium. Measured values of wall static pressure p_5 fall within this region, implying the flow is in thermochemical equilibrium. However, the pitot pressure, which is directly proportional to free-stream density, generally falls between predictions for an equilibrium expansion and for a frozen expansion. Similar trends were also observed for the pilot-model expansion tube as reported in reference 1. The present results demonstrate the inadequacies of the simple flow models considered in reference 9 for describing the complex thermochemical-gas dynamic aspects of the test flow.

Representative pitot-pressure profiles obtained with the four-probe survey rake are shown in figure 14. These results were obtained with heated helium driver gas and double-diaphragm mode of operation. The values for the pitot pressure were taken at 100 μsec after interface arrival. For the lower values of p_1 shown in figure 14, corresponding to interface velocities of 5.3 to 6.2 km/sec, the test core appears to be roughly 6 to 8 cm in diameter or approximately one-half the tube diameter. At the higher values of p_1, which correspond to a much lower value of interface velocity, the existence of an inviscid test core is questionable. The relatively large probe spacing of the pitot-pressure survey rake does not provide the resolution required for accurate determination of test-core diameter for this case. If a test core does exist, the diameter will be less than about 4 cm.

Test time in the expansion-tube flow is defined as the period of quasi-steady pitot pressure following the arrival of the interface at the test section. The test times for the runs reported herein, as inferred from measured-pitot-pressure time histories, varied from 200 to 400 μsec. In general, test times inferred from pressure histories were in good agreement with calculated (ref. 9) test times at the higher interface velocities. However, runs at the lower interface velocities indicated a decrease in pitot pressure before the arrival of the expansion fan, thereby reducing the test times by 100 to 200 μsec. This same decrease in pitot pressure and corresponding decrease in test time were also observed in the pilot-model expansion tube (ref. 1).

CONCLUSIONS

A general description of the Langley 6-inch expansion tube is presented along with discussion of the basic components, internal resistance heater, arc-discharge assemblies,

instrumentation, and operating procedure. Preliminary results using unheated and resistance-heated helium as the driver gas at pressures from approximately 17 to 59 MPa and temperatures from 300 to 510 K, air as the test gas, and helium as the acceleration gas yield the following conclusions:

1. Measured incident shock velocities in the driven section exceeded simple, real-air shock-tube theory. Shock velocities for heated-helium driver gas were greater than those for unheated helium, as expected, but the difference between these velocities was significantly less than predicted.

2. For the present driven section length of 2.44 m, the incident shock in this section was still accelerating upon arrival at the secondary diaphragm station. The test-air–helium-acceleration-gas interface was observed to initially accelerate, then attenuate by approximately 150 m/sec in a distance of 14 m.

3. Comparison of measured wall static pressures to simple expansion-tube theory implies a thermochemical equilibrium expansion. A similar comparison of the predicted pitot pressures shows experimental results fall between predicted equilibrium and frozen-flow expansions. Thus, the thermochemical state of the test flow may not be inferred from simple expansion-tube theory.

4. For interface velocities from about 5 to 6 km/sec, pitot-pressure surveys indicated a test core diameter of approximately one-half the tube diameter. The existence of an inviscid test core at the lower values of interface velocities is questionable.

5. Test times, which ranged from 200 to 400 μsec, were in good agreement with theory except at the lower interface velocities. At these lower velocities, a dip in the pitot pressure was observed prior to arrival of the expansion fan at the test section, thereby significantly reducing the test time.

Langley Research Center
National Aeronautics and Space Administration
Hampton, Va. 23665
June 6, 1975

REFERENCES

1. Jones, Jim J.; and Moore, John A.: Exploratory Study of Performance of the Langley Pilot Model Expansion Tube With a Hydrogen Driver. NASA TN D-3421, 1966.
2. Trimpi, Robert L.: A Preliminary Theoretical Study of the Expansion Tube, A New Device for Producing High-Enthalpy Short-Duration Hypersonic Gas Flows. NASA TR R-133, 1962.
3. Friesen, Wilfred J.: Use of Photoionization in Measuring Velocity Profile of Free-Stream Flow in Langley Pilot Model Expansion Tube. NASA TN D-4936, 1968.
4. Weilmuenster, K. James: An Experimental Investigation of Wall Boundary-Layer Transition Reynolds Numbers in an Expansion Tube. NASA TN D-7541, 1974.
5. Mechtly, E. A.: The International System of Units - Physical Constants and Conversion Factors (Second Revision). NASA SP-7012, 1973.
6. Nealy, John E.: Performance and Operating Characteristics of the Arc-Driven Langley 6-Inch Shock Tube. NASA TN D-6922, 1972.
7. Yamaki, Yoshio; and Rooker, James R.: Experimental Investigation of Circular, Flat, Grooved and Plain Steel Diaphragms Bursting Into a 30.5-Centimeter-Square Section. NASA TM X-2549, 1972.
8. Creel, Theodore R., Jr.: Experimental Performance of an Internal Resistance Heater for Langley 6-Inch Expansion Tube Driver. NASA TN D-7070, 1972.
9. Miller, Charles G., III; and Wilder, Sue E.: Program and Charts for Determining Shock Tube, Expansion Tube, and Expansion Tunnel Flow Quantities for Real Air. NASA TN D-7752, 1975.
10. Laney, Charles C., Jr.: Microwave Interferometry Technique for Obtaining Gas Interface Velocity Measurements in an Expansion Tube Facility. NASA TM X-72625, 1974.
11. Mauldin, Lemual E., III; and Compton, E. Conrad: An Optical System for Recording Schlieren Images With a Continuous-Writing Ultra-High-Speed Framing Camera. NASA TN D-4986, 1969.
12. White, Donald R.: Influence of Diaphragm Opening Time on Shock-Tube Flows. J. Fluid Mech., vol. 4, pt. 6, Nov. 1958, pp. 585-599.
13. Satofuka, Nobuyuki: A Numerical Study of Shock Formation in Cylindrical and Two-Dimensional Shock Tubes. ISAS Rep. No. 451, Univ. of Tokyo, 1970.
14. Curzon, F. L.; and Phillips, M. G. R.: Low Attenuation Shock Tube: Driving Mechanism and Diaphragm Characteristics. Canadian J. Phys., vol. 49, no. 15, Aug. 1, 1971, pp. 1982-1993.

15. Olstad, Walter B.; Kemper, Jane T.; and Bengtson, Roger D.: Equilibrium Normal-Shock and Stagnation-Point Properties of Helium for Incident Shock Mach Numbers From 1 to 30. NASA TN D-4754, 1968.

16. Mirels, Harold: Test Time in Low-Pressure Shock Tubes. Phys. Fluids, vol. 6, no. 9, Sept. 1963, pp. 1201-1214.

TABLE 1.– INSTRUMENTATION STATIONS

Station locations for present tests		Modified station locations for future reference	
Station	Distance from primary diaphragm, m	Station	Distance from primary diaphragm, m
1	0.3085	1	0.3085
2	.861	2	.861
3	1.365	3	1.365
4	1.657	4	1.657
5	1.822	5	1.822
6	2.110	6	2.110
7	2.297	7	2.297
8	8.041	8	3.507
9	10.779	9	3.811
10	13.045	10	4.1175
11	15.248	11	4.248
12	17.450	12	4.412
13	19.737	13	4.575
End of tube	21.600	14	6.943
Window	21.778	15	8.065
		16	9.194
		17	9.358
		18	9.521
		19	10.780
		20	13.045
		21	15.2485
		22	17.450
		23	19.737
		Collar	21.612
		Window	21.778

TABLE 2.– TEST CONDITIONS

p_4, MPa	p_1, kPa	T_4/T_1	$M_{s,1}$	p_{10}, Pa	U_5, km/sec
17.2	1.72	1.4 to 1.6	8.3 to 8.50	3.3 to 66.7	5.48 to 6.20
17.2	3.44	1.6 to 1.7	7.55 to 7.75	13.3 to 66.7	5.30 to 5.77
33.8	3.44	1.4 to 1.6	8.35 to 8.54	6.6 to 133	5.54 to 6.72
33.8	6.89	1.6 to 1.7	7.9 to 8.25	13.3 to 66.5	5.80 to 6.56
58.5	48.3	1.6	6.6	931	3.78
55.0	68.9	1.6	6.2	931	3.78
[a]19.5	6.89	1.0	6.3		
[a]24.5	6.89	1.0	6.3		
[a]34.5	3.45	1.0	6.96		
17.2	3.45	1.0	7.0 to 7.2		
33.8	3.45	1.0	7.6 to 7.7		

[a]Shock-tube runs with a single steel diaphragm.

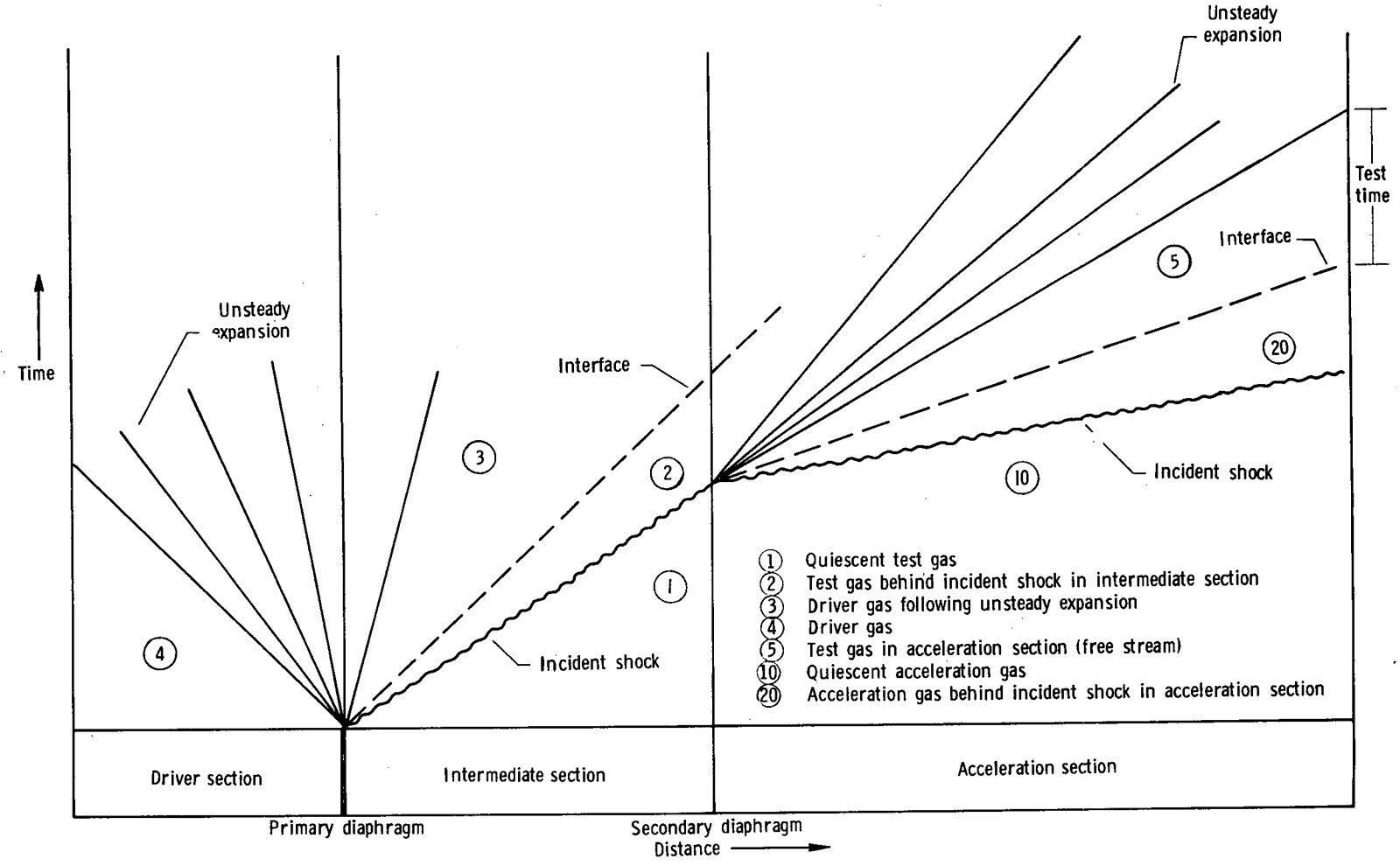

Figure 1.– Schematic diagram of expansion-tube flow sequence.

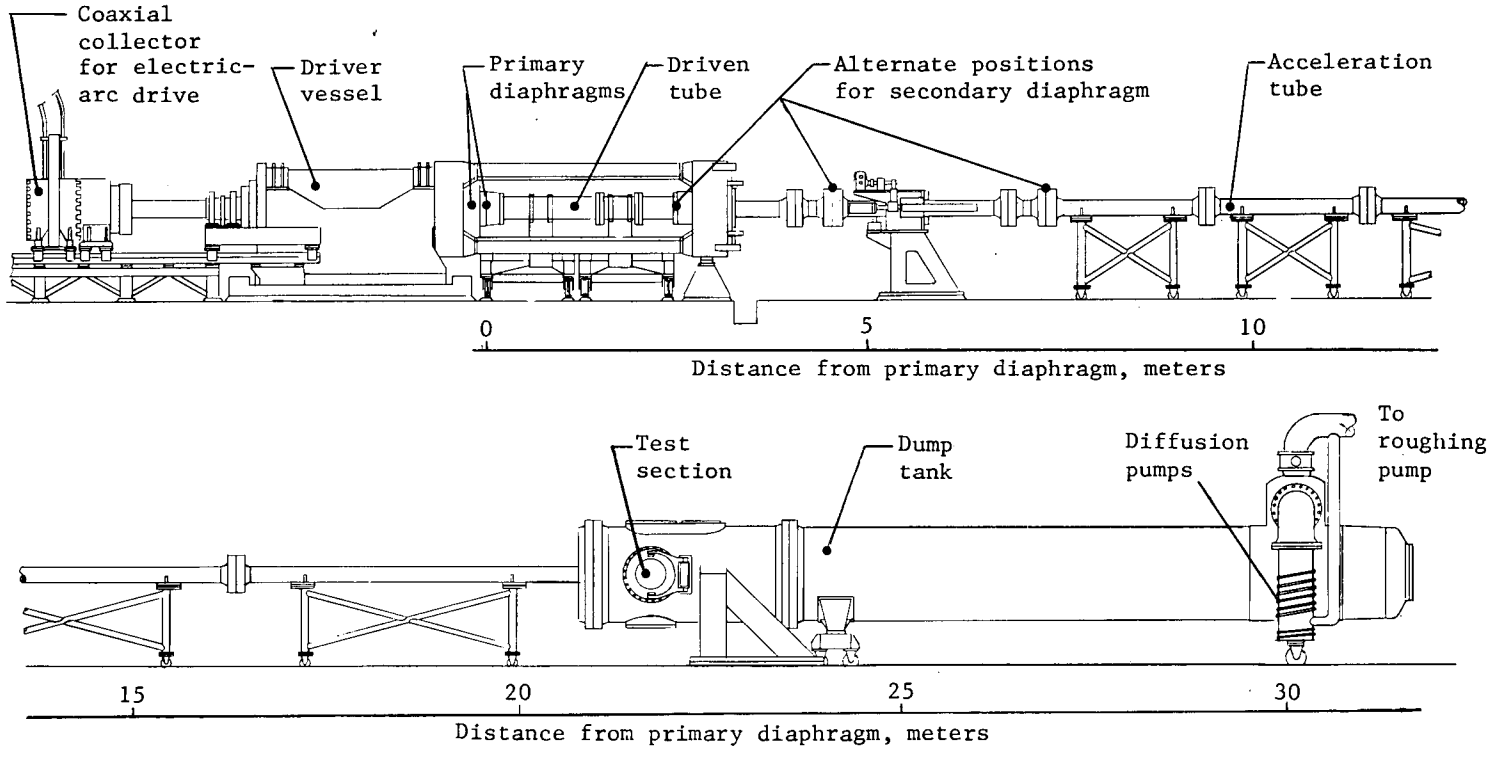

Figure 2.– Sketch of Langley 6-inch expansion tube.

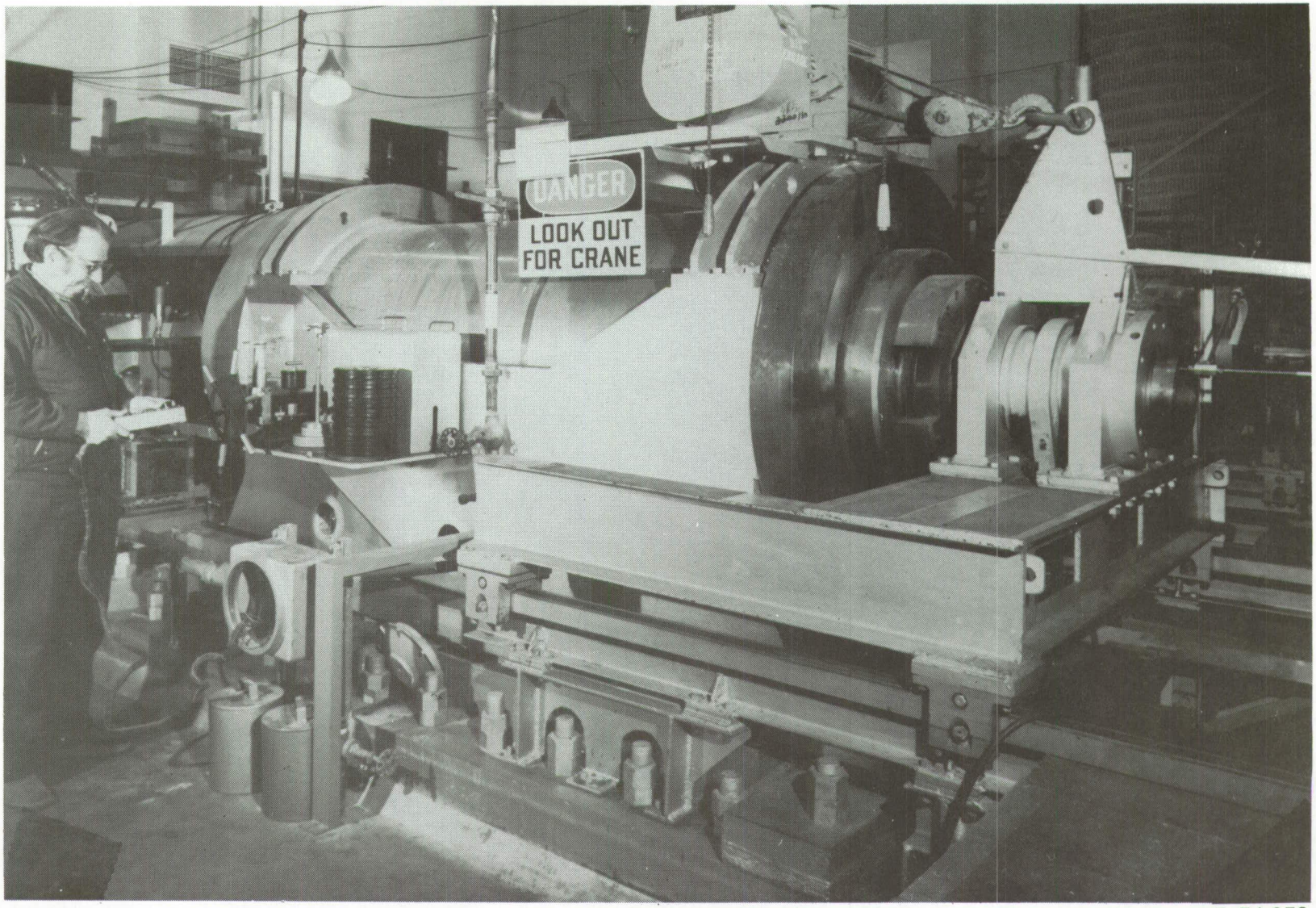

L-74-379

(a) High-pressure driver vessel.

Figure 3.– Photographs of basic components of the Langley 6-inch expansion tube.

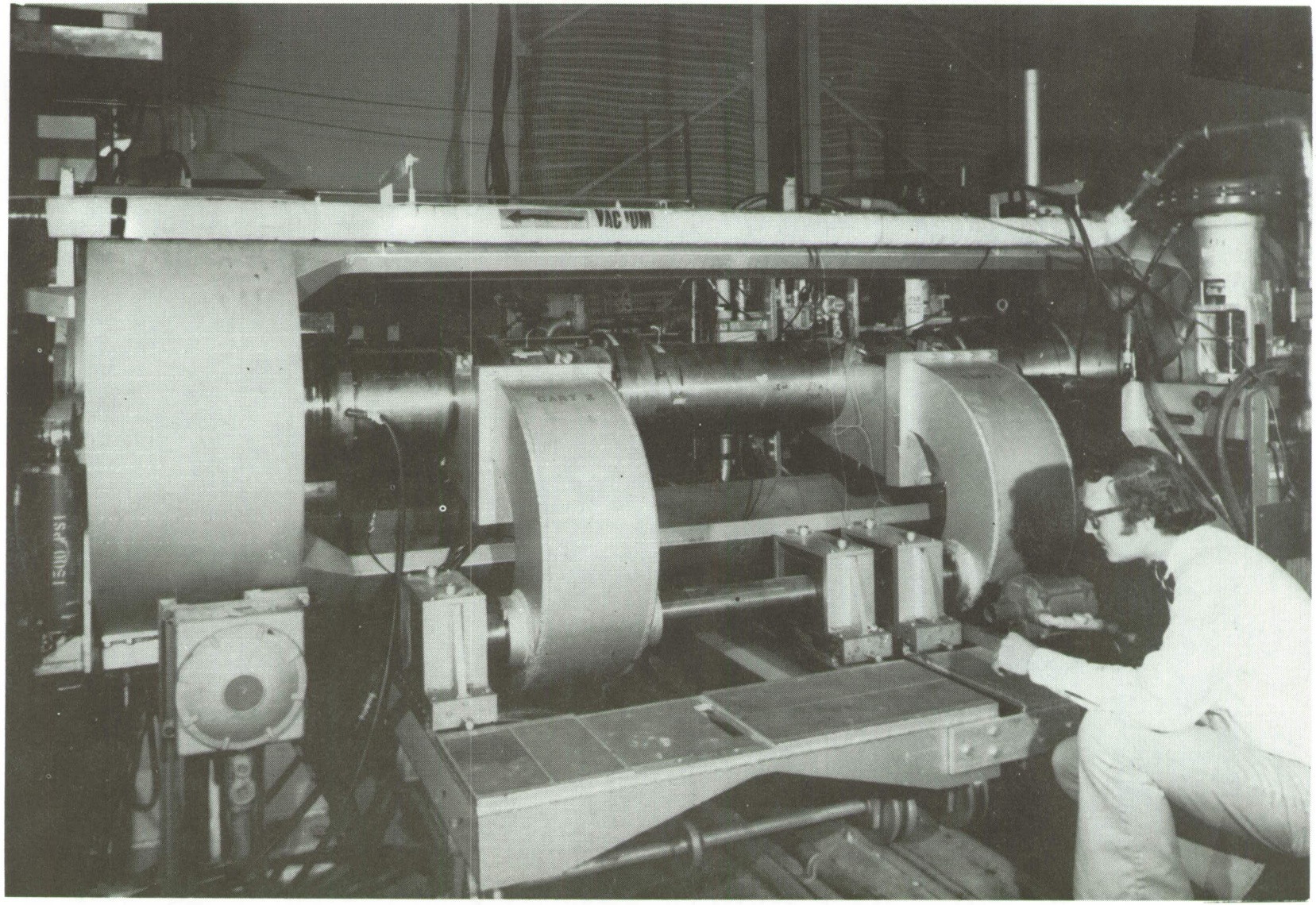

L-74-380

(b) Driven tube or intermediate section.

Figure 3.– Continued.

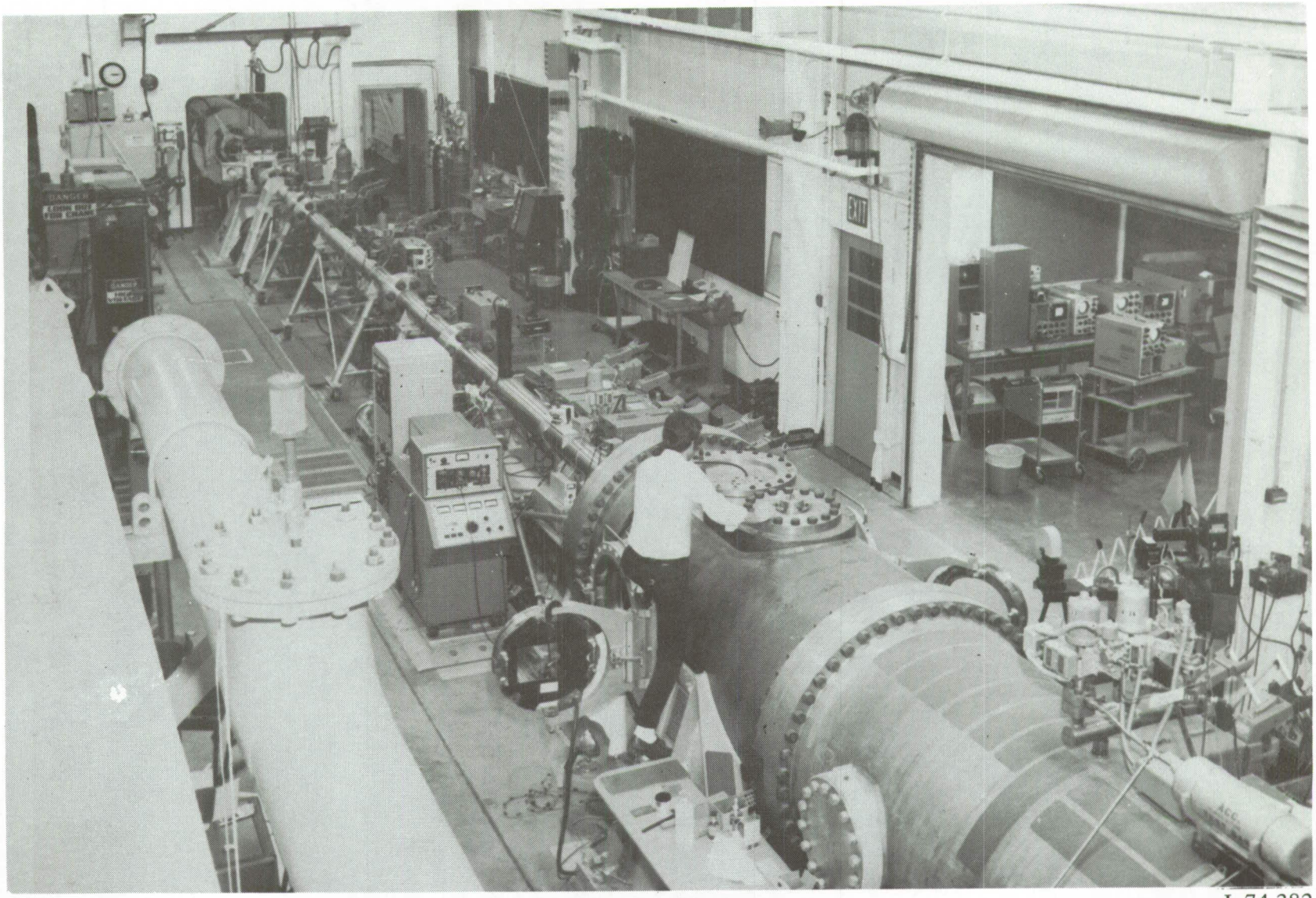

L-74-382

(c) Acceleration section and dump tank.

Figure 3.– Continued.

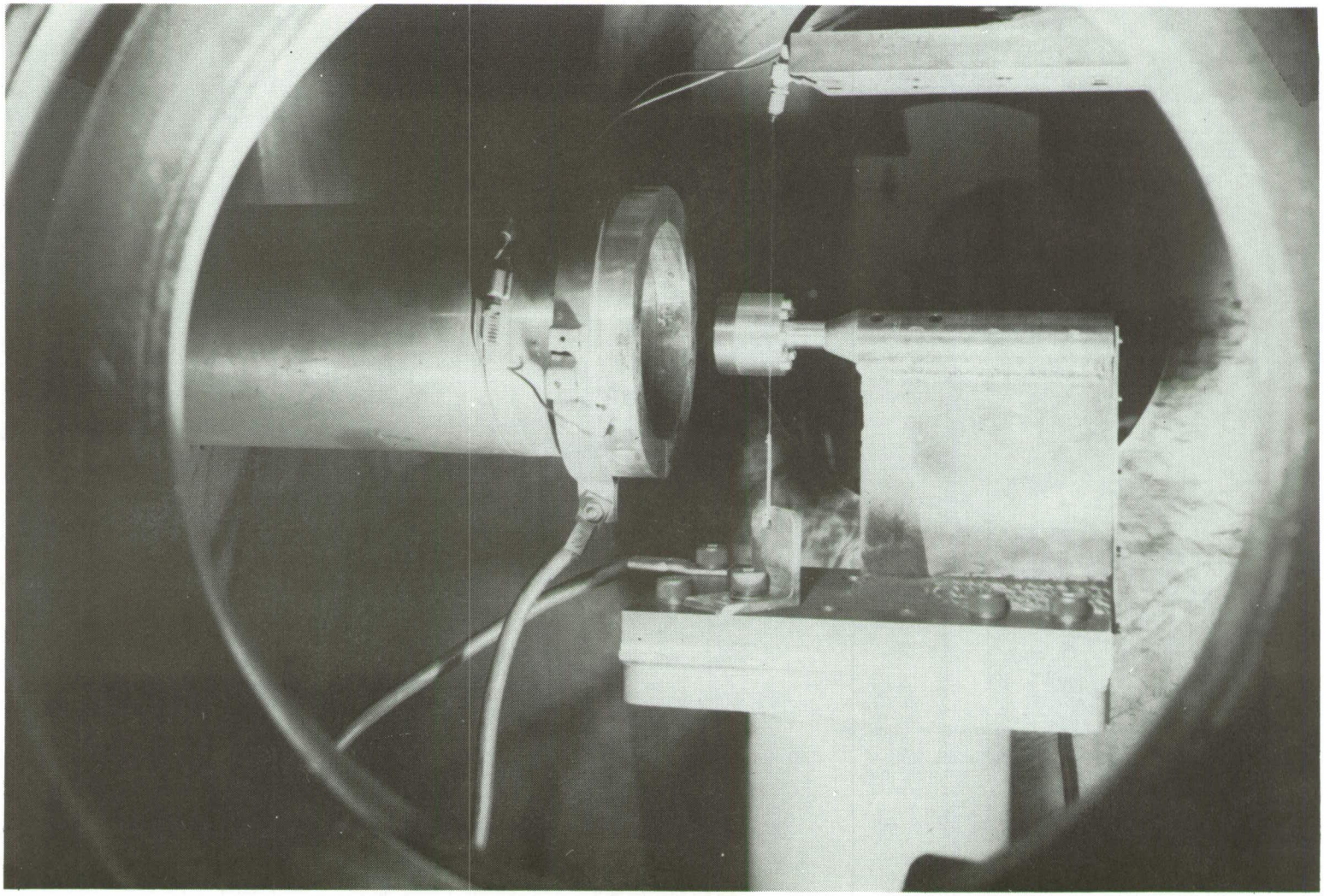

L-74-381

(d) Test section with typical model and microwave antenna installed.

Figure 3.- Concluded.

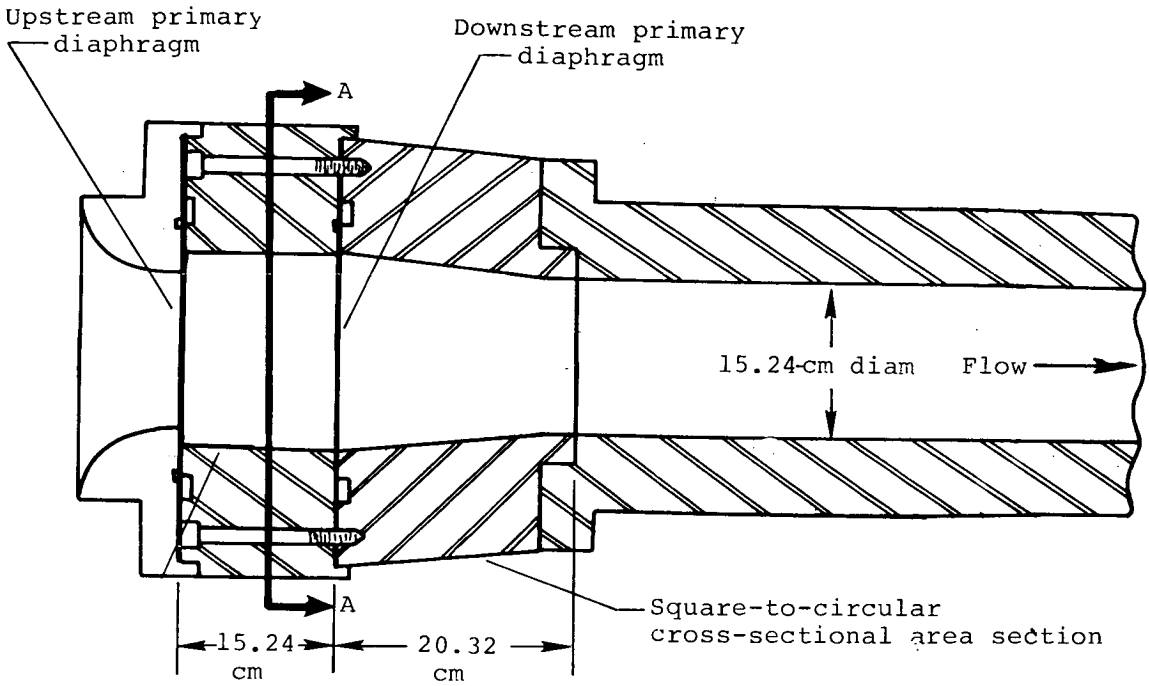

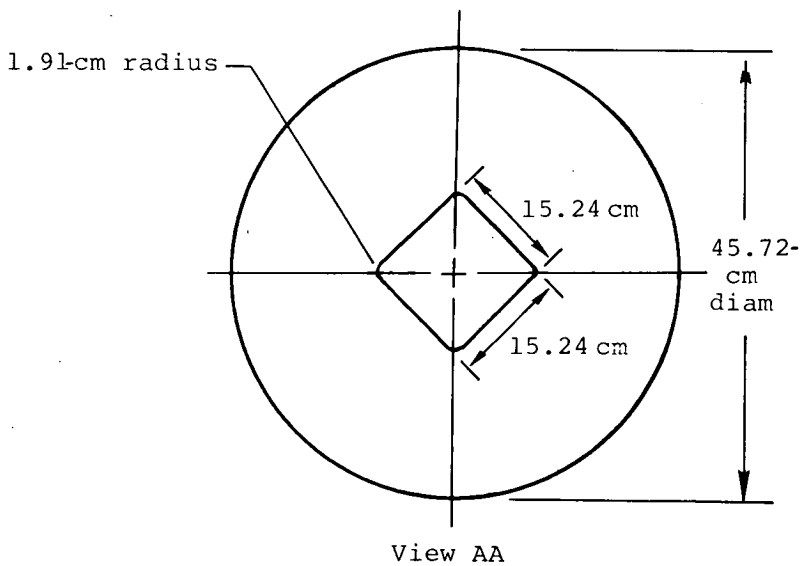

Figure 4.– Sketch of double-diaphragm section and intermediate section.

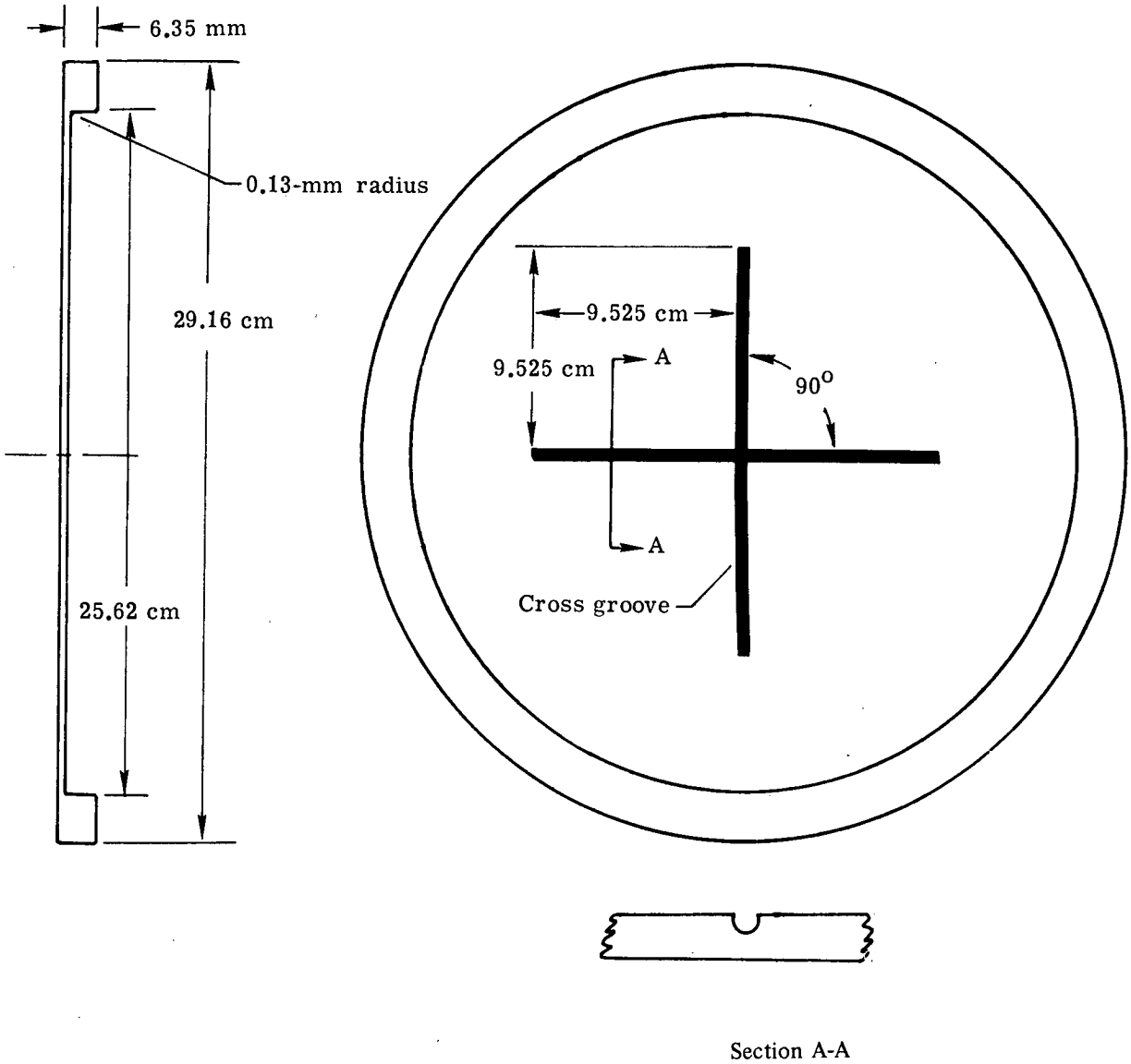

Figure 5.– Diaphragm geometry. Diaphragm material is AISI Type 304 stainless steel.

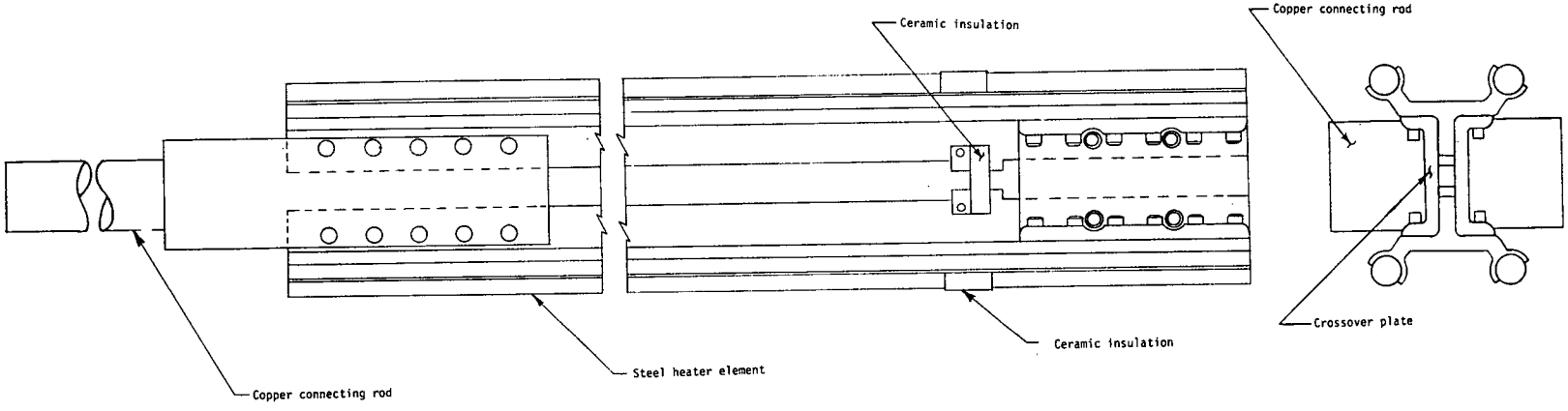

Figure 6.– Electrical resistance heating element for the Langley 6-inch expansion tube driver (from ref. 8).

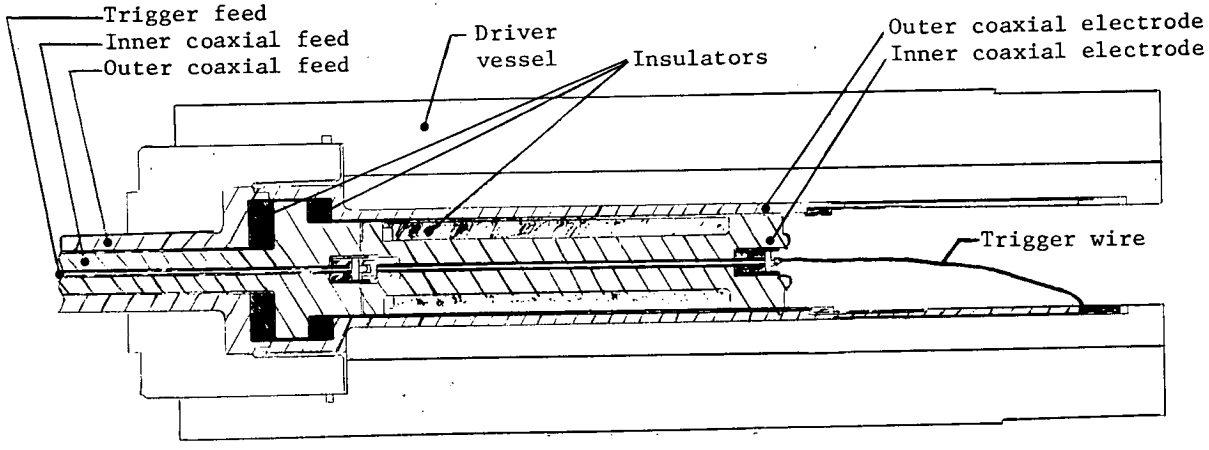

(a) Coaxial configuration.

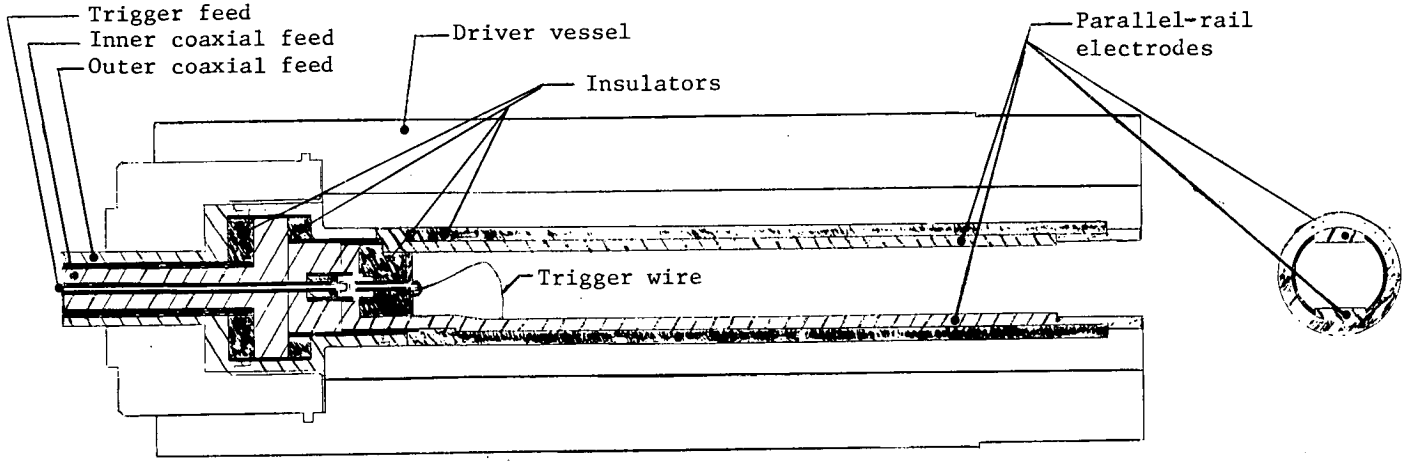

(b) Parallel-rail configuration.

Figure 7.– Sketch of electric-arc driver configurations.

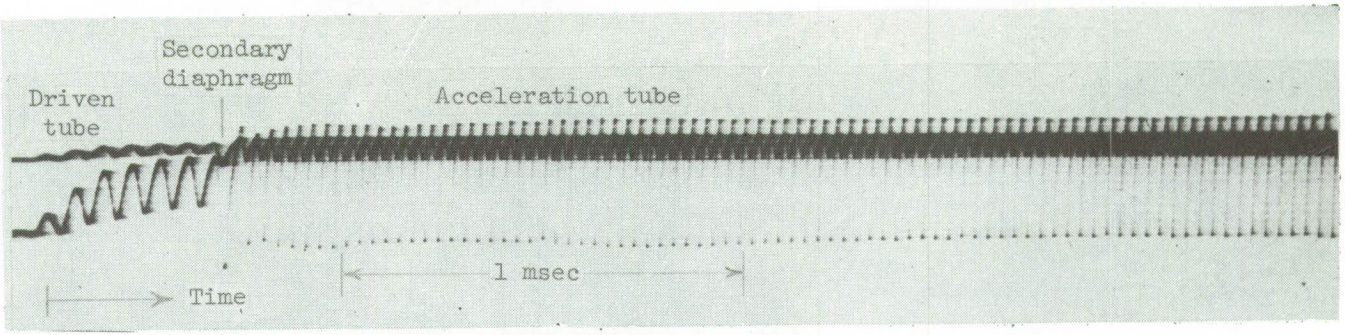

(a) Microwave record.

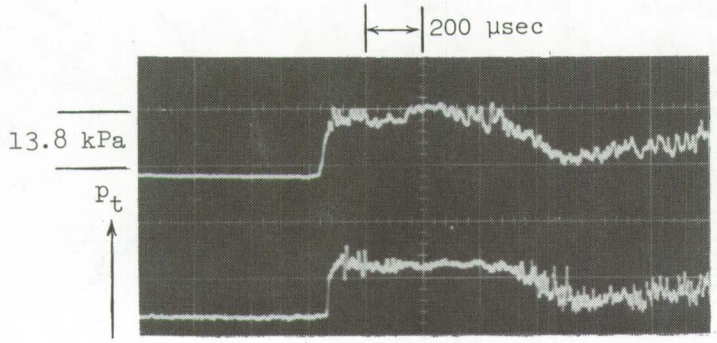

(b) Pitot pressure.

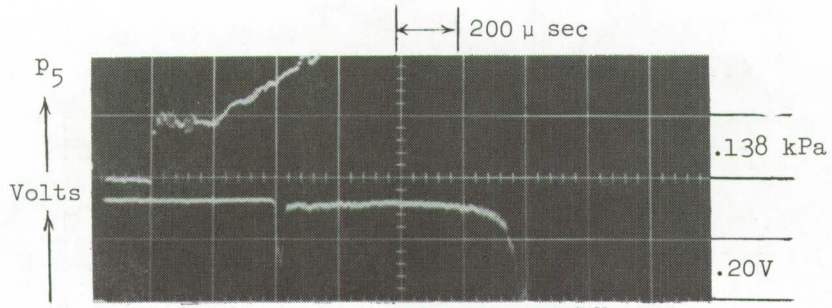

(c) Wall static pressure and photomultiplier, at stations 13.0 m and 15.2 m, respectively.

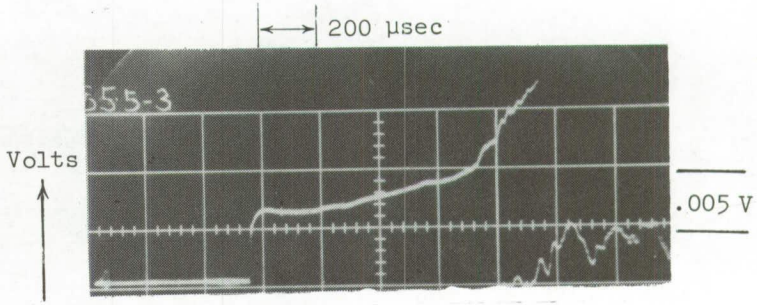

(d) Heat transfer at station 15.2 m.

L-75-173

Figure 8.- Representative oscilloscope traces of several flow quantities.

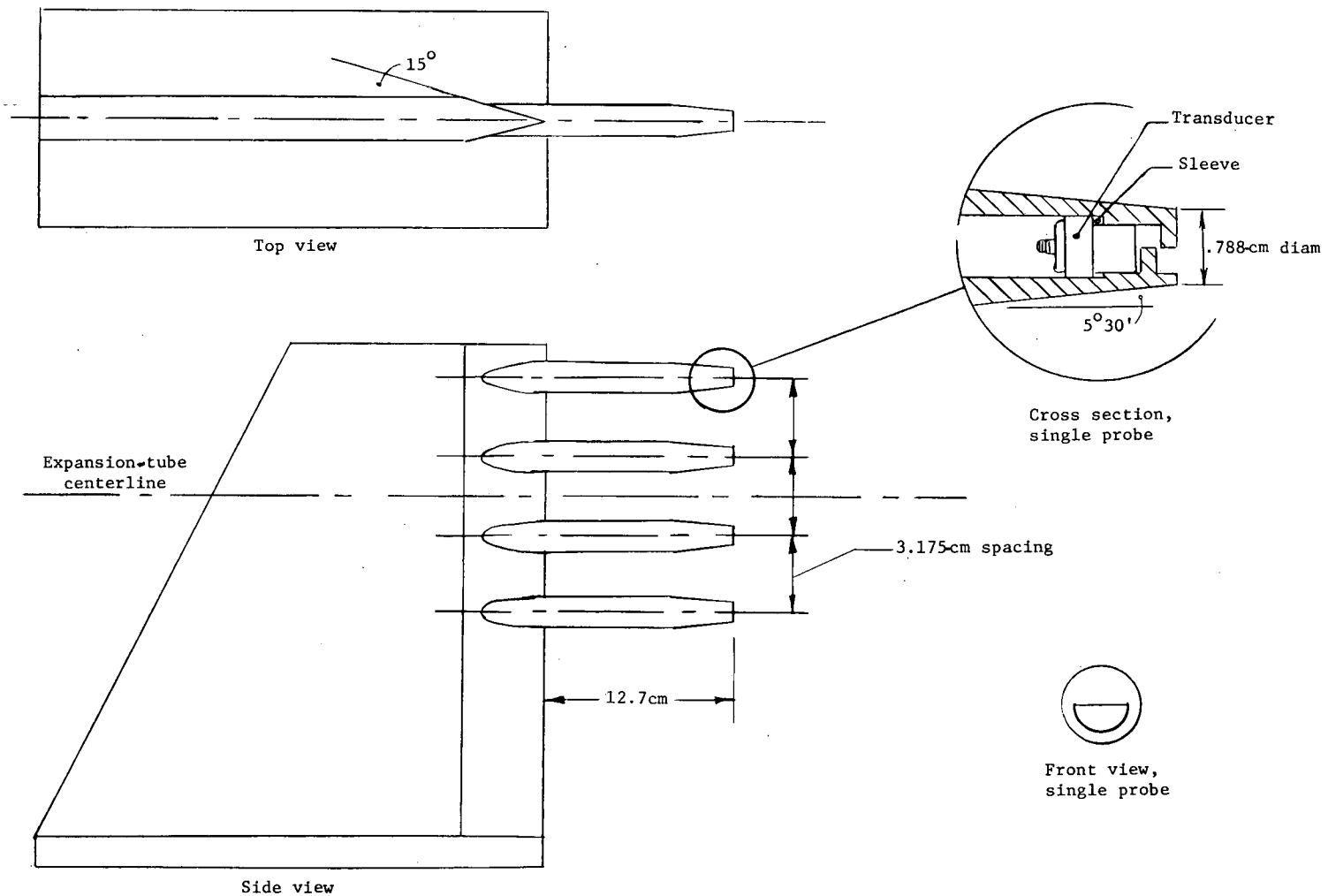

Figure 9.– Pitot-pressure survey rake.

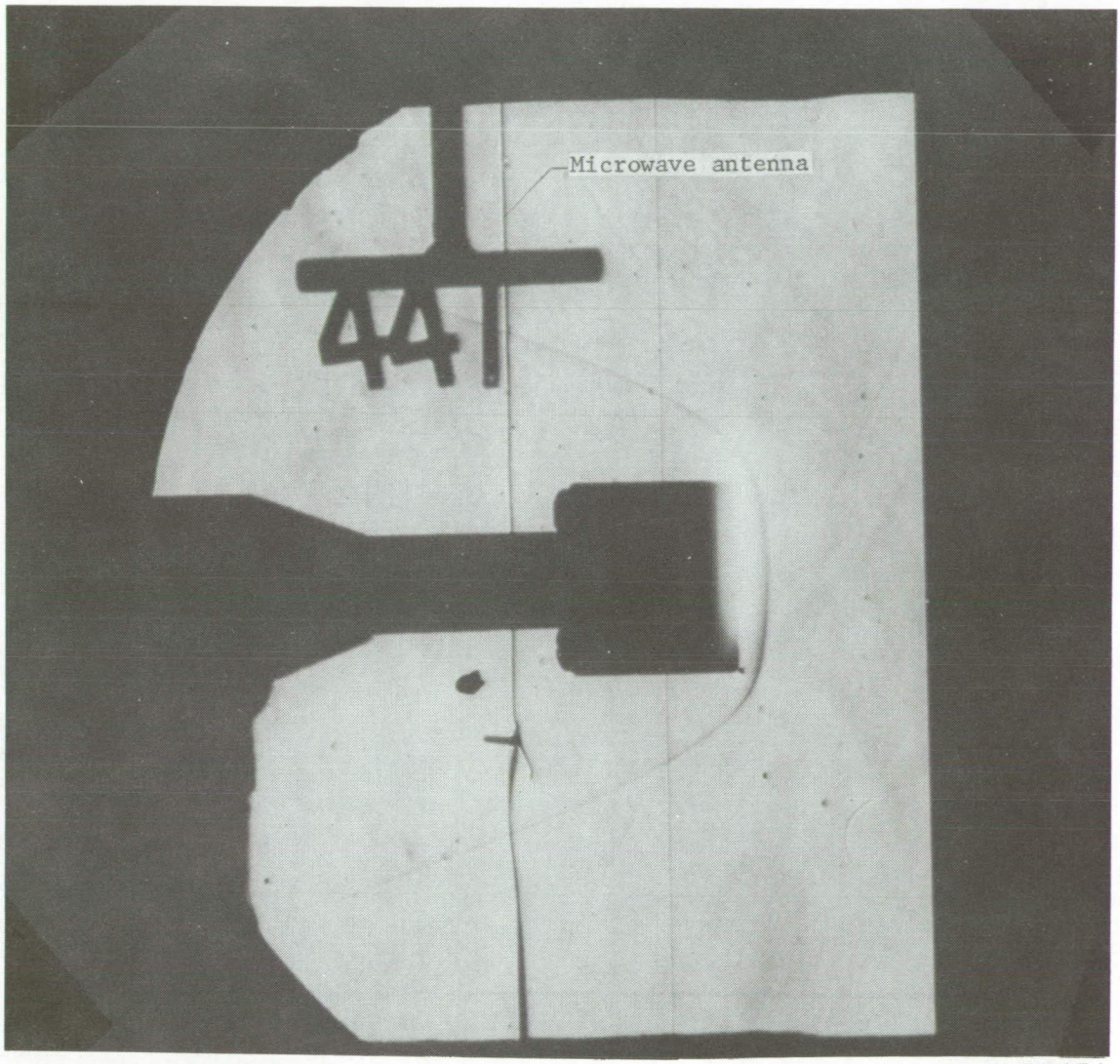

L-75-174

Figure 10.– Schlieren photograph illustrating shock about a blunt body in Mach 7.7 airflow.

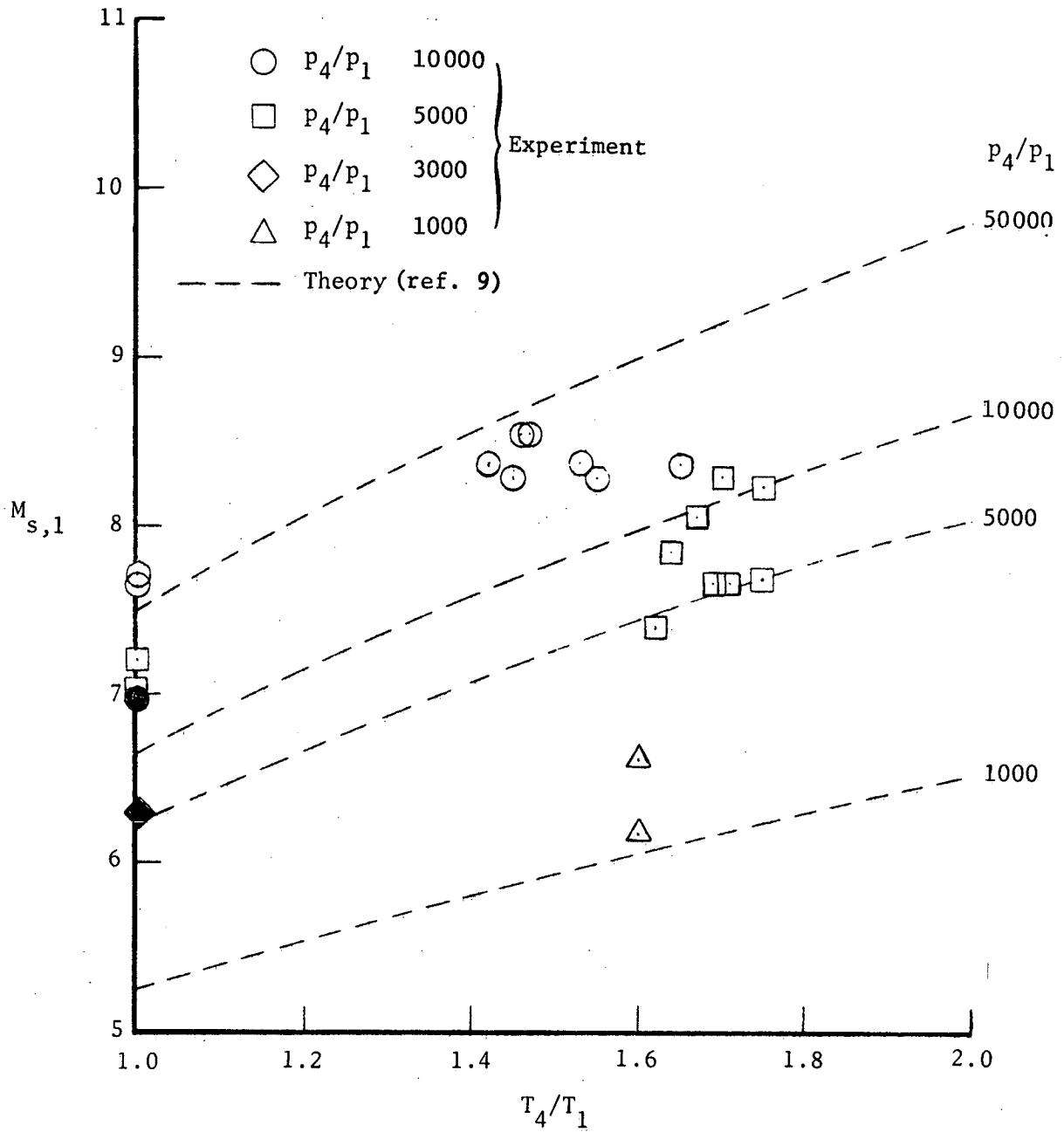

Figure 11.– Comparison of measured shock Mach numbers in the driven section to theory for helium driver gas and air test gas. Open symbols denote double diaphragm; closed symbols denote single diaphragm.

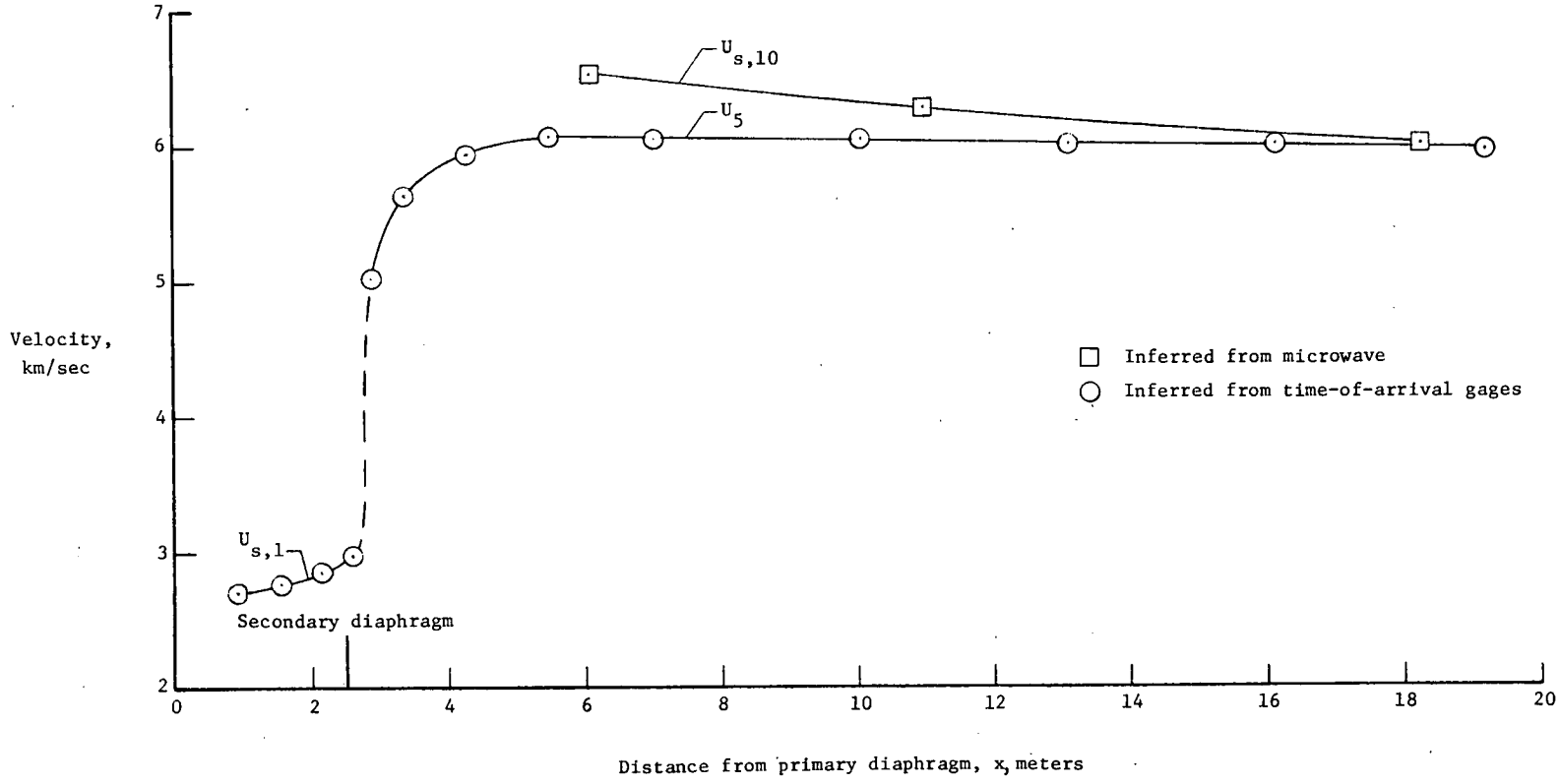

Figure 12.– Incident shock velocity and interface velocity as a function of distance downstream of primary diaphragm. Helium driver gas; air test gas; $p_4/p_1 = 9416$; $p_1 = 3.5$ kPa; $T_4/T_1 = 1.65$; double diaphragm.

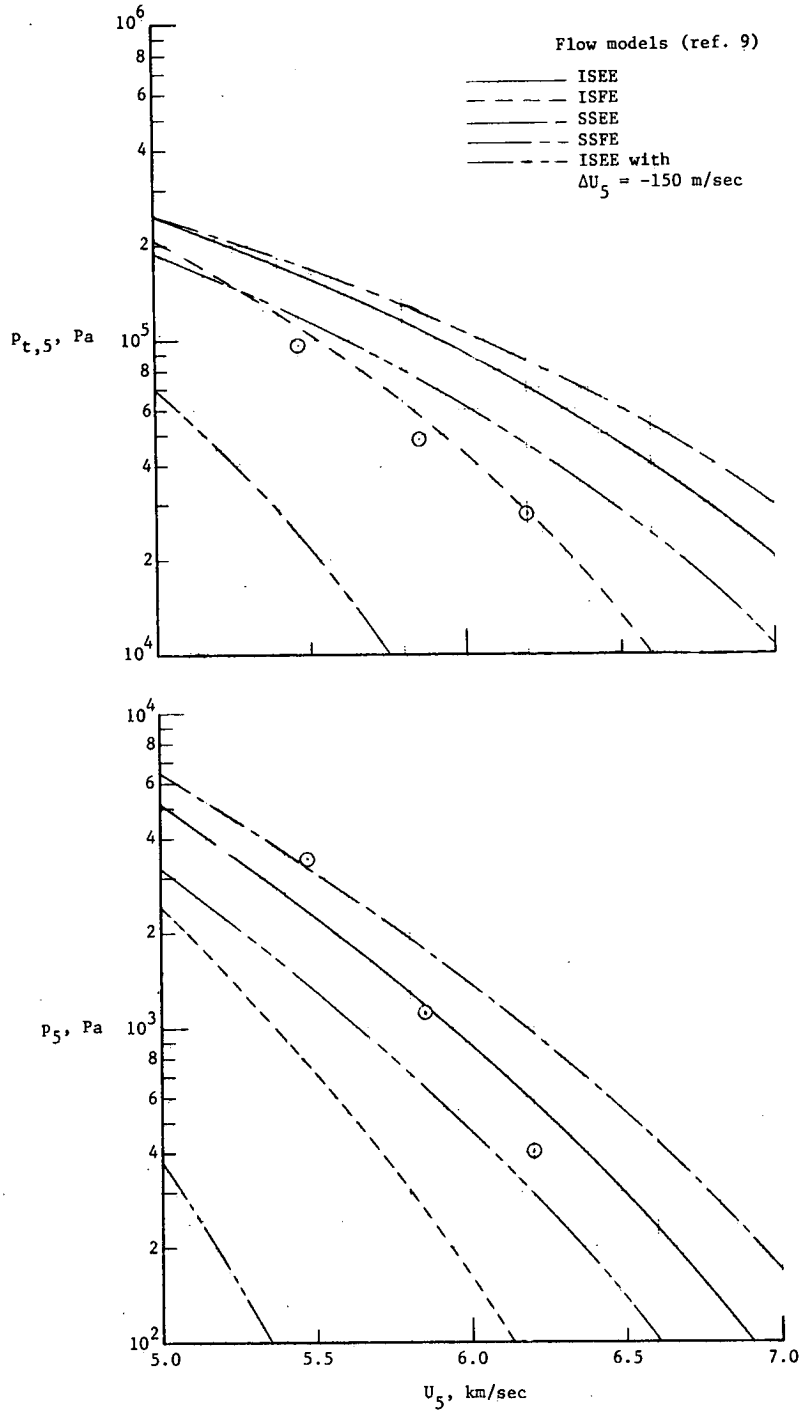

(a) p_1 = 1.72 kPa; p_4/p_1 = 10 000.

Figure 13.– Comparison of measured values of wall static pressure and pitot pressure with theory for heated helium driver gas and air test gas. (Circles denote experimental data.)

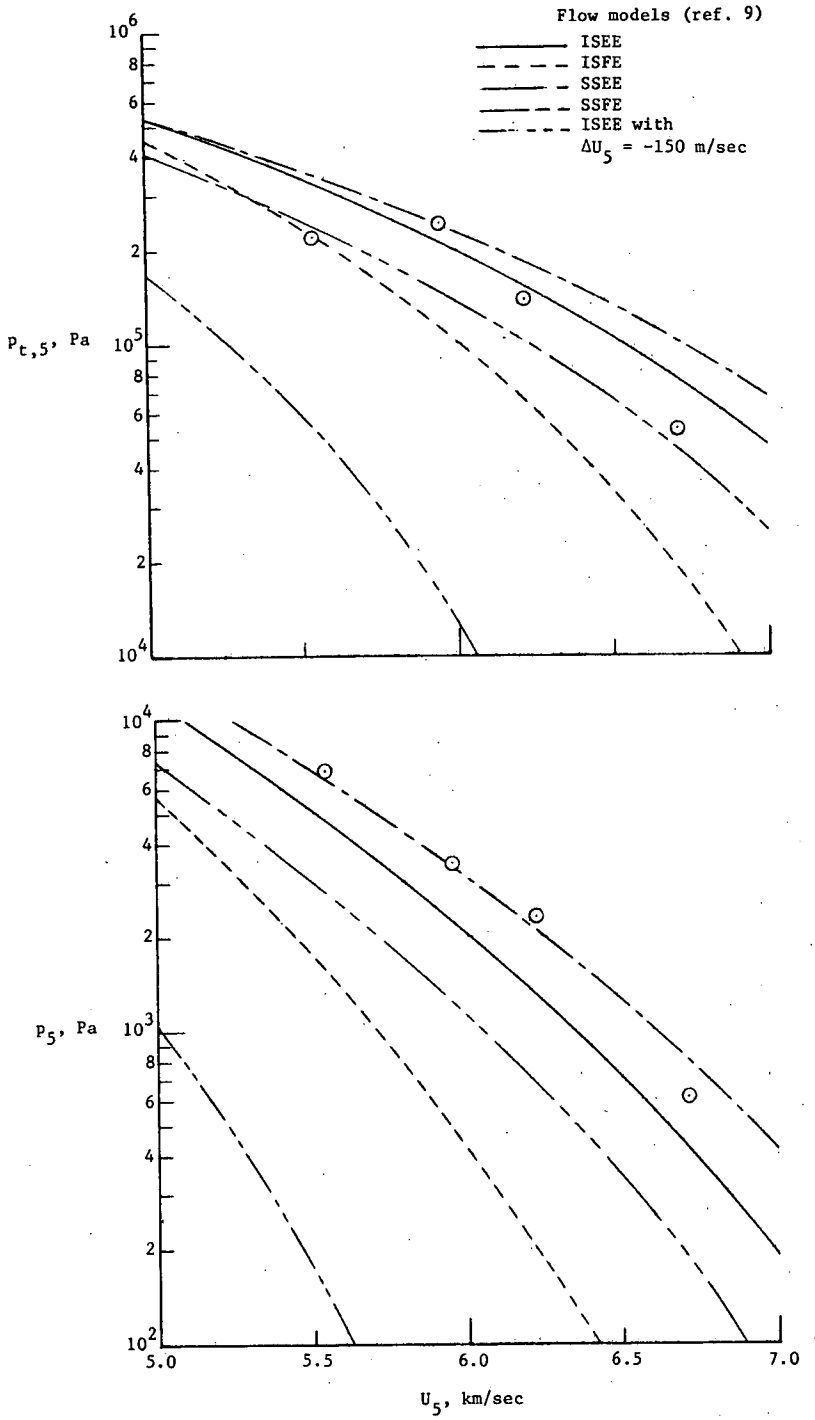

(b) p_1 = 3.44 kPa; p_4/p_1 = 9800.

Figure 13.- Continued.

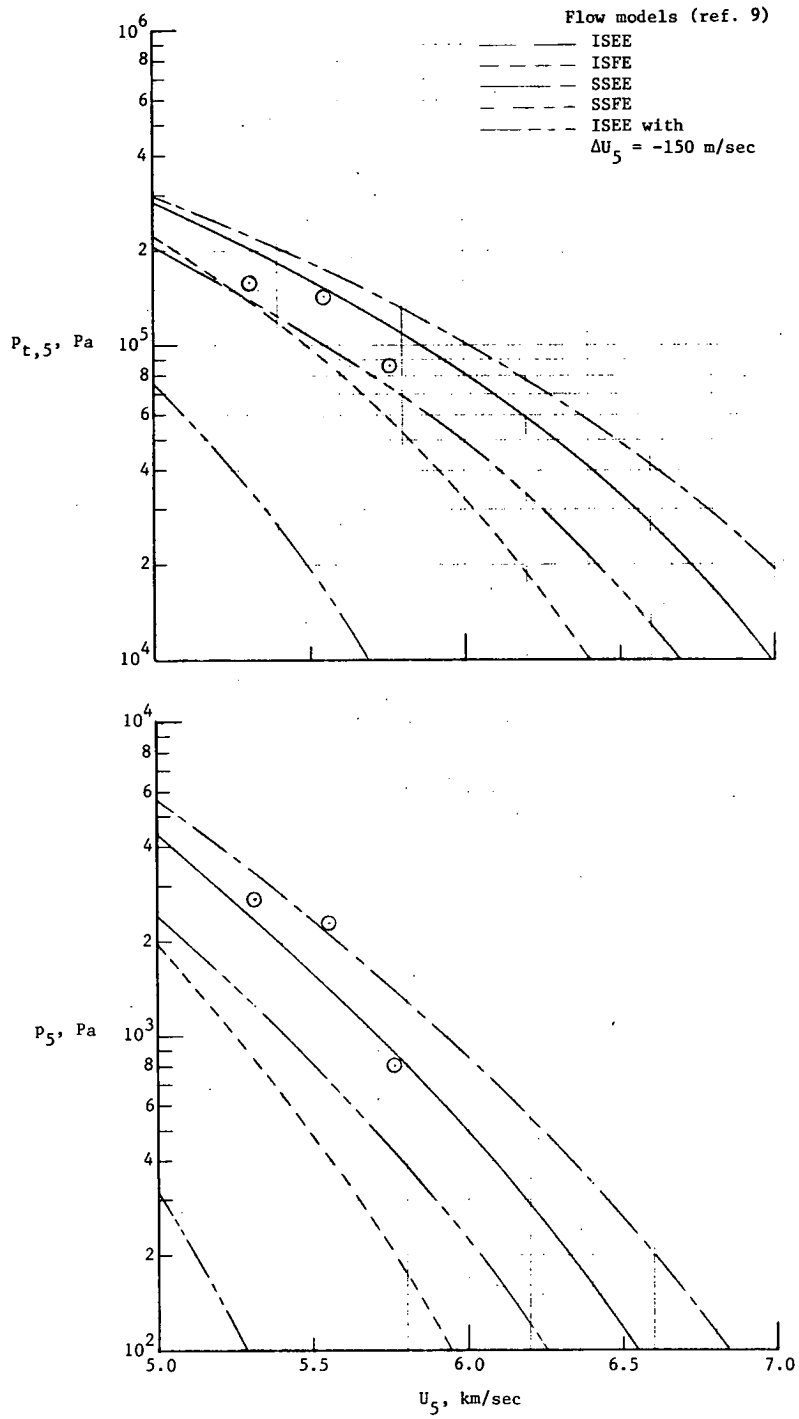

(c) p_1 = 3.44 kPa; p_4/p_1 = 4900.

Figure 13. Continued.

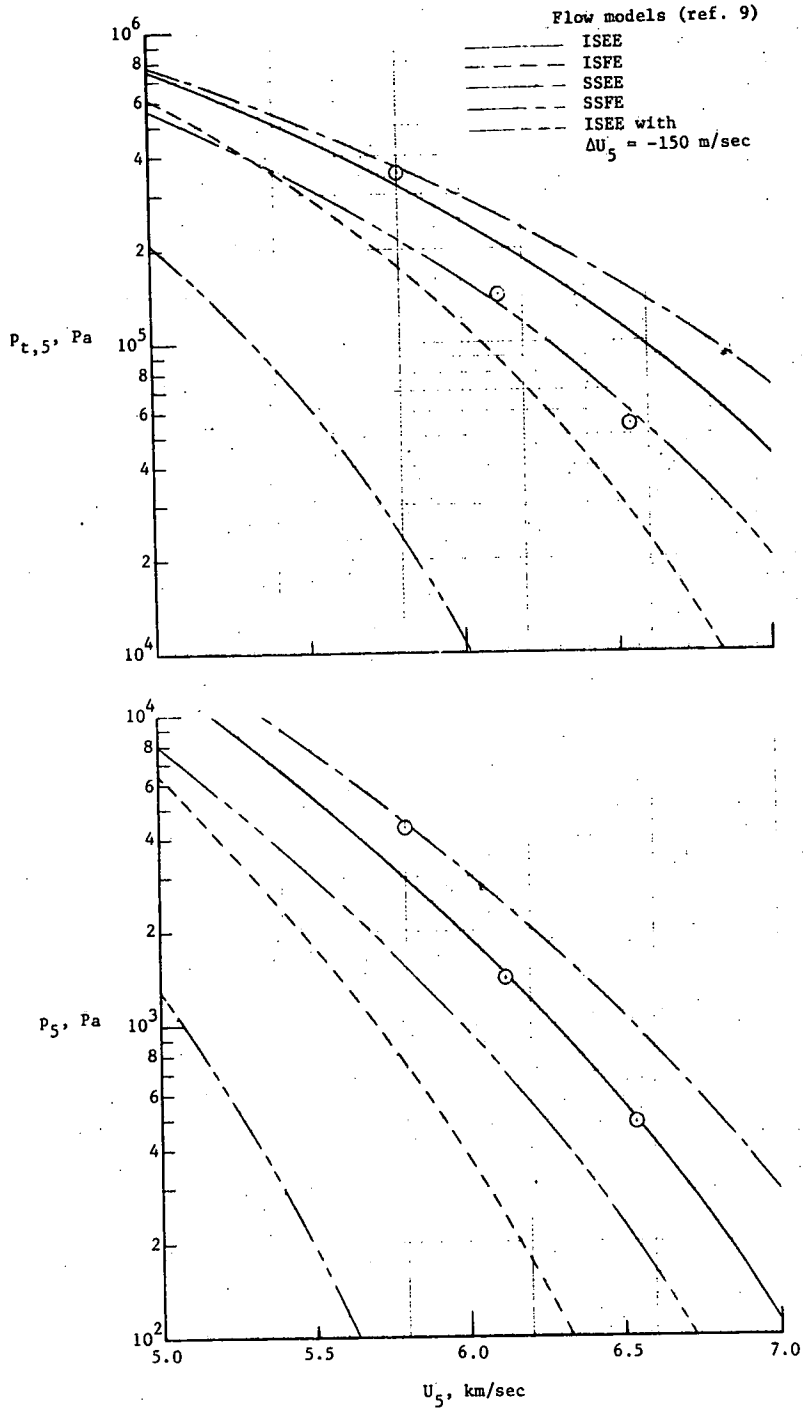

(d) p_1 = 6.89 kPa; p_4/p_1 = 4900.

Figure 13.- Continued.

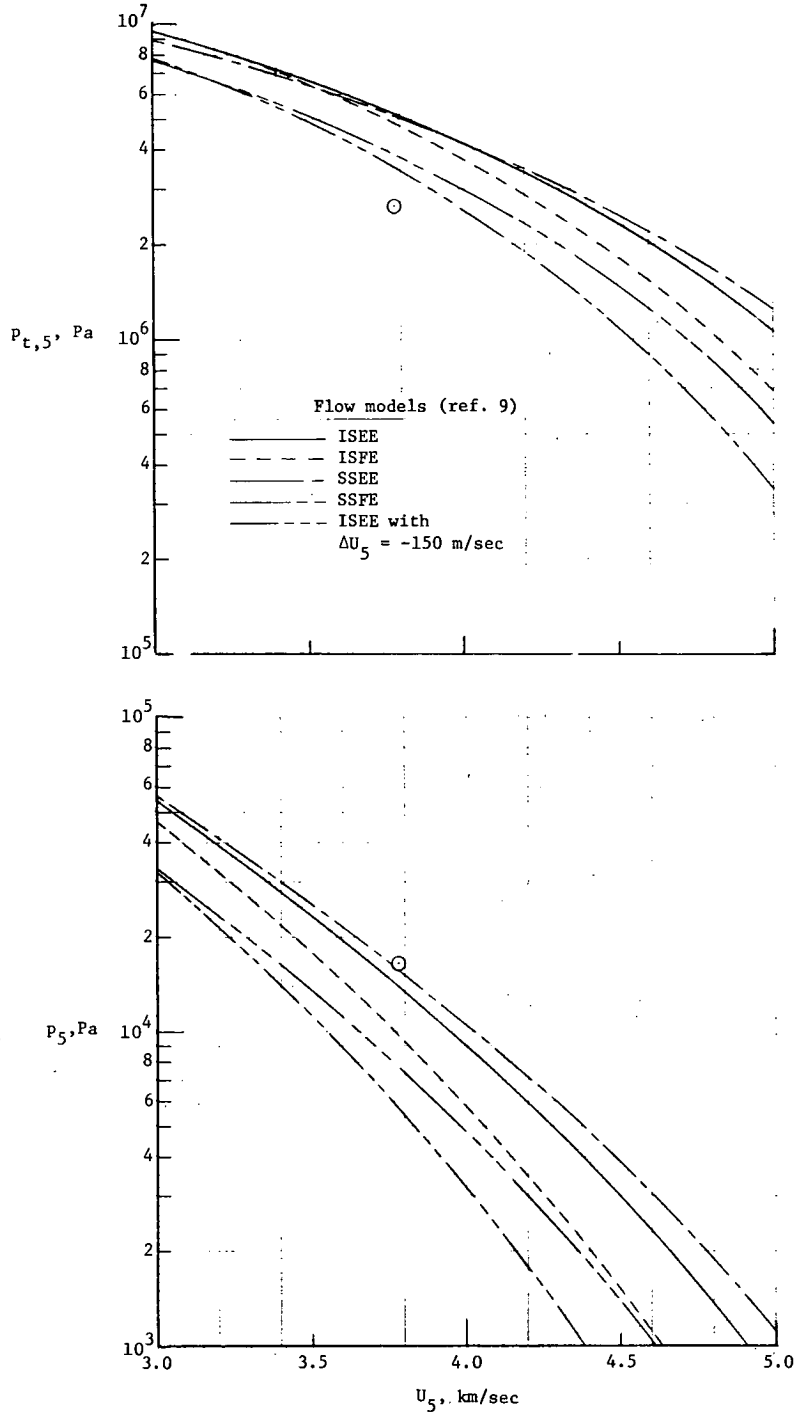

(e) p_1 = 48.3 kPa; p_4/p_1 = 1200.

Figure 13.- Continued.

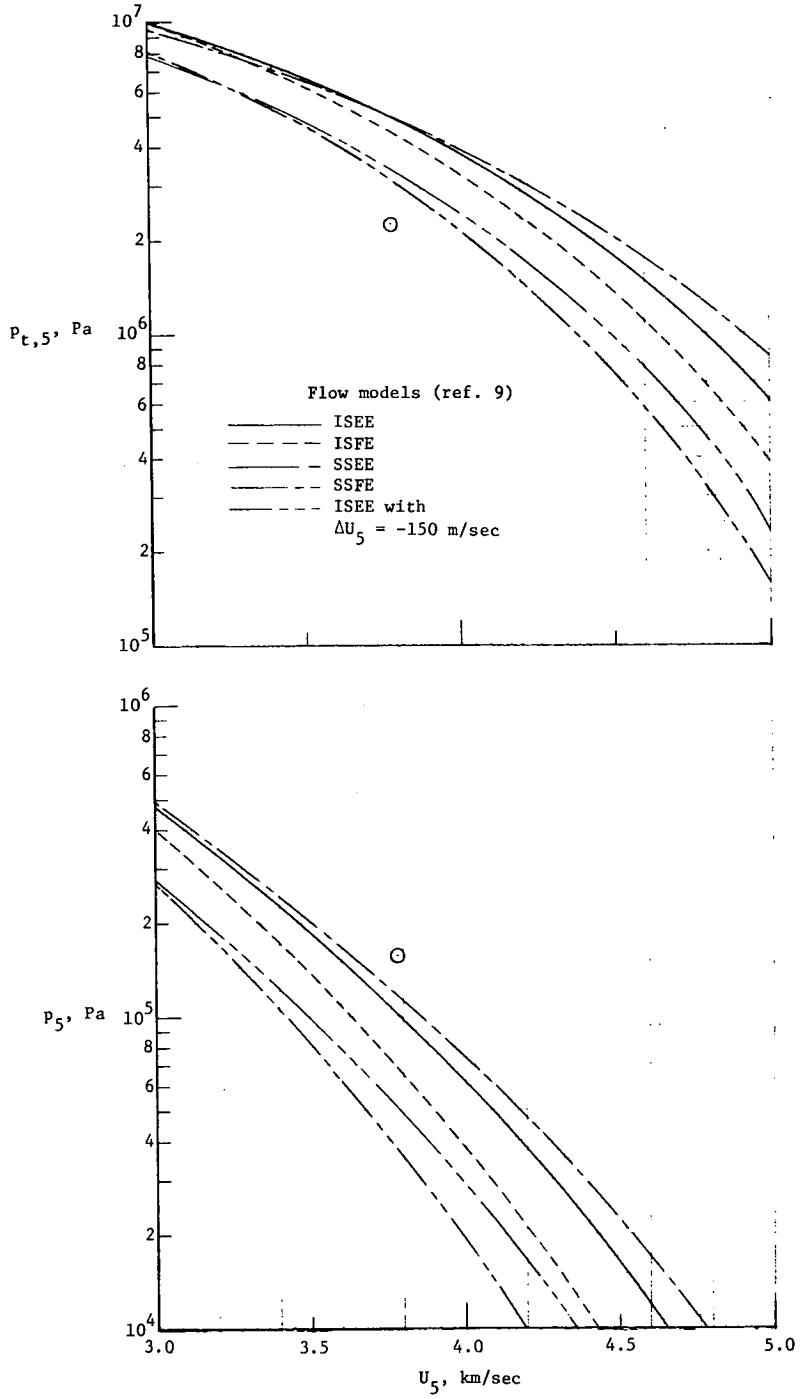

(f) p_1 = 68.9 kPa; p_4/p_1 = 800.

Figure 13.- Concluded.

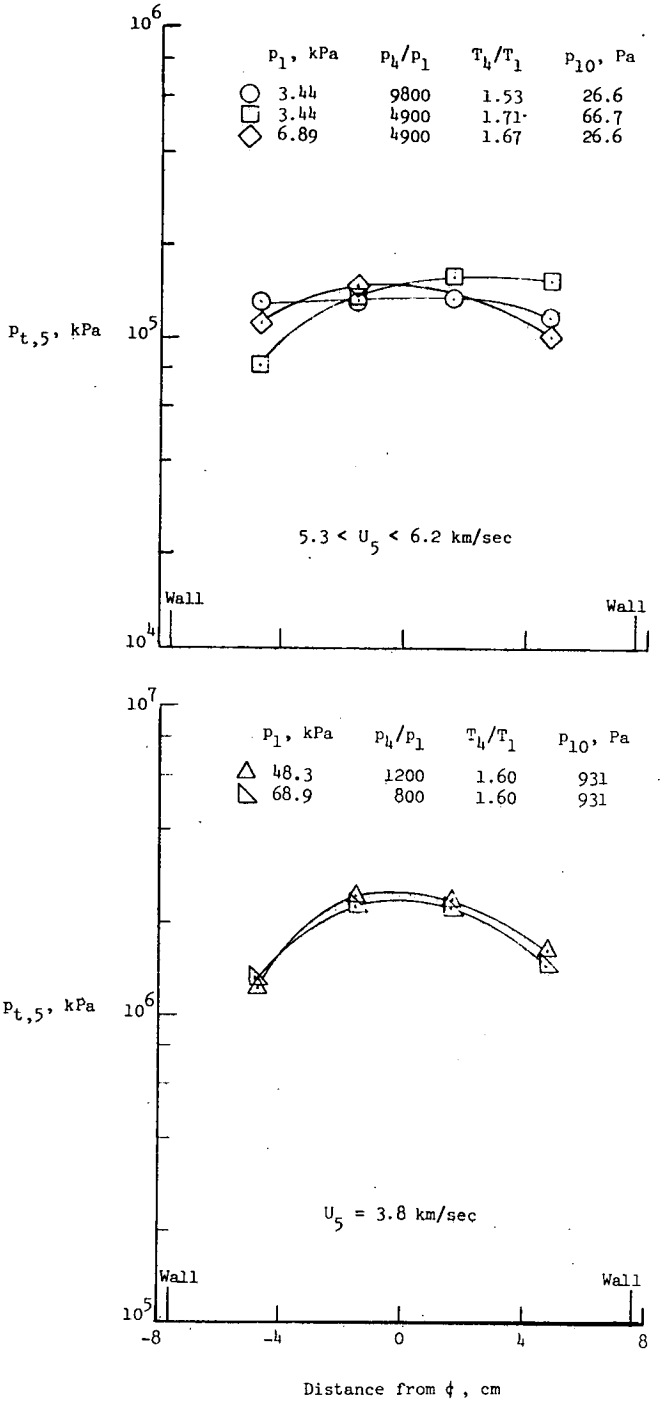

Figure 14.– Measured pitot-pressure profiles for heated helium driver gas, air test gas, and helium acceleration gas at two interface velocities.

NATIONAL AERONAUTICS AND SPACE ADMINISTRATION
WASHINGTON, D.C. 20546

OFFICIAL BUSINESS
PENALTY FOR PRIVATE USE $300

SPECIAL FOURTH-CLASS RATE BOOK

POSTAGE AND FEES PAID
NATIONAL AERONAUTICS AND SPACE ADMINISTRATION
451

U.S.MAIL

POSTMASTER: If Undeliverable (Section 158 Postal Manual) Do Not Return

"The aeronautical and space activities of the United States shall be conducted so as to contribute . . . to the expansion of human knowledge of phenomena in the atmosphere and space. The Administration shall provide for the widest practicable and appropriate dissemination of information concerning its activities and the results thereof."

—NATIONAL AERONAUTICS AND SPACE ACT OF 1958

NASA SCIENTIFIC AND TECHNICAL PUBLICATIONS

TECHNICAL REPORTS: Scientific and technical information considered important, complete, and a lasting contribution to existing knowledge.

TECHNICAL NOTES: Information less broad in scope but nevertheless of importance as a contribution to existing knowledge.

TECHNICAL MEMORANDUMS: Information receiving limited distribution because of preliminary data, security classification, or other reasons. Also includes conference proceedings with either limited or unlimited distribution.

CONTRACTOR REPORTS: Scientific and technical information generated under a NASA contract or grant and considered an important contribution to existing knowledge.

TECHNICAL TRANSLATIONS: Information published in a foreign language considered to merit NASA distribution in English.

SPECIAL PUBLICATIONS: Information derived from or of value to NASA activities. Publications include final reports of major projects, monographs, data compilations, handbooks, sourcebooks, and special bibliographies.

TECHNOLOGY UTILIZATION PUBLICATIONS: Information on technology used by NASA that may be of particular interest in commercial and other non-aerospace applications. Publications include Tech Briefs, Technology Utilization Reports and Technology Surveys.

Details on the availability of these publications may be obtained from:

SCIENTIFIC AND TECHNICAL INFORMATION OFFICE

NATIONAL AERONAUTICS AND SPACE ADMINISTRATION

Washington, D.C. 20546